Applied Catalysis B: Environmental 199 (2016) 108–122

Contents lists available at ScienceDirect

Applied Catalysis B: Environmental

journal homepage: www.elsevier.com/locate/apcatb

Selective hydrogenation using palladium bioinorganic catalyst

Ju Zhu [a], Joseph Wood [a], Kevin Deplanche [b], Iryna Mikheenko [b], Lynne E. Macaskie [b,*]

[a] School of Chemical Engineering, University of Birmingham, Edgbaston, Birmingham B15 2TT, UK
[b] School of Biosciences, University of Birmingham, Edgbaston, Birmingham B15 2TT, UK

ARTICLE INFO

Article history:
Received 13 February 2016
Received in revised form 22 May 2016
Accepted 24 May 2016
Available online 3 June 2016

Keywords:
Palladium
Bacteria
Hydrogenation
Isomerisation
2-pentyne
Soybean oil

ABSTRACT

Palladium bioinorganic catalyst (bio-Pd) was manufactured using bacteria (*Desulfovibrio desulfuricans and Escherichia coli*) *via* the reduction of Pd(II) to bio-scaffolded Pd(0) nanoparticles (NPs). The formed Pd NPs were examined using electron microscopy and X-ray powder diffraction methods: a loading of 5 wt% Pd showed an average particle size of ~4 nm. The catalytic activities of the prepared bio-Pd NPs on both bacteria were compared in two hydrogenation reactions with that of a conventionally supported Pd catalyst (Pd/Al_2O_3). Concentration profiles of the different hydrogenation products were fitted using a Langmuir-Hinshelwood expression. In 2-pentyne hydrogenation, 5 wt% $Pd_{E.coli}$ achieved 100% of 2-pentyne conversion in 20 mins and produced $10.1 \pm 0.7 \times 10^{-2}$ mol L^{-1} of desired *cis*-2-pentene; in contrast 5 wt% Pd/Al_2O_3 yielded $6.5 \pm 0.4 \times 10^{-2}$ mol L^{-1} of *cis*-2-pentene after 40 mins. In the solvent-free hydrogenation of soybean oil, the use of 5 wt% $Pd_{E.coli}$ yielded *cis*-C18:1 of 1.03 ± 0.04 mol L^{-1} and *trans*-C18:1 of 0.26 ± 0.03 mol L^{-1} (~50% less of the latter than 5 wt% Pd/Al_2O_3) after 5 h. Similar results were obtained using bio-$Pd_{E.coli}$ and bio-$Pd_{D.desulfuricans}$. Bio-Pd was concluded to have the advantage of a lower *cis-trans* isomerisation in hydrogenation of alkyne/alkenes. Hence biomanufacturing is an environmentally attractive, scalable and facile alternative to conventional heterogeneous catalyst for application in industrial hydrogenation processes. *D. desulfuricans* is inconvenient to grow at scale but wastes of *E. coli* are produced from various industrial processes. 'Second life' (i.e. recycled from a pilot scale biohydrogen production process) *E. coli* cells were used to make bio-Pd catalysts. Although 'bio-$Pd_{secondlife'}$ gave a slower conversion rate of 2-pentyne and soybean oil compared to bio-Pd from purpose-grown cells it showed a higher selectivity to the *cis*-isomer product.

1. Introduction

Many heterogeneous metal catalysts (rhodium, palladium, platinum, ruthenium and nickel) exhibit high activity in the hydrogenation of carbon-carbon double and triple bonds. Nanoparticulate palladium, due to its high hydrogen adsorption capacity [1], is one of the most important hydrogenation catalysts used industrially. Conventionally, a support such as alumina, silica, zeolites, silica-alumina and various forms of carbon (charcoal, activated carbon) is used to prepare Pd-catalyst, of which metallic nanoparticles (NPs) of less than 5 nm diameter are desirable due to their high activity [2]. Various synthetic strategies have been applied to prepare such NPs, *e.g.* polyol-based [3,4] and seed-mediated growth [5] methods. The size and morphology of Pd-NPs depend strongly on conditions such as pH, temperature, and the type of metallic precursor and stabiliser. Preparation of stabilisers can be complicated, *e.g.* in the case of complex ligand synthesis, which requires specialist equipment or the use of an inert atmosphere [see 6], while classical synthetic strategies require the use of a series of reductants, which are often toxic and/or expensive [see 7]. This study evaluates novel palladium catalyst in the form of highly ordered Pd-NPs on biomolecular templates [7,8], taking advantage of the ability of bacteria to sorb precious metal ions (*e.g.* Pd(II)), which are then reduced *via* hydrogenase activity (*via* H_2 as the electron donor) into crystalline NPs embedded into the bacterial surface (*e.g.* on *Desulfovibrio desulfuricans* or *Escherichia coli*) [8–10] which serves as a scaffold stabilising the NPs against agglomeration [11] and with very high specific surface areas [12]. For example, discrete Pd(0) NPs of ~5 nm diameter were synthesised on *D. desulfuricans* ('bio-$Pd_{D.desulfuricans}$') [13], concurrently stabilised against agglomeration and retained for re-use [11]. Uniform coverage of small (5–10 nm) Pd NPs on the cell surface of *E. coli* ('bio-$Pd_{E.coli}$') at a loading of 5 wt% Pd was reported Deplanche et al. [14], with comparable catalytic activity to bio-$Pd_{D.desulfuricans}$ [15]. Offering, potentially, particle size and shape control (a dominant requirement in industrial application) the microbial method has provided an effective route for

* Corresponding author.
E-mail address: L.E.Macaskie@bham.ac.uk (L.E. Macaskie).

http://dx.doi.org/10.1016/j.apcatb.2016.05.060

synthesising NPs [16–19], recoverable for re-use with minimal loss of activity [11] or for continuous use as biofilm-immobilised catalyst [20]. Taking into account also the need to conserve primary resources and recycle precious metals, by applying this biotechnological approach, effective bionanocatalyst can be sourced from metal-containing wastes [21,22], potentially providing a low-cost route to nanocatalyst production with low environmental impact. The precious metal can be easily and economically recovered from the used catalyst by incineration, sonication or microwaving the biomass [6].

In order to impact significantly upon the long-established field of palladium-catalysis [23] a new formulation must be: (i) economic to manufacture at scale; (ii) free of addition of toxic or expensive chemicals and need for high temperature; (iii) more effective in bulk or niche applications than traditional catalysts and (iv) recoverable for re-use without attrition or loss. Bio-Pd, comprising individual Pd-NPs held on a micron sized carrier (the bacterial cell) [11] and bio-adhering onto support matrices [20] fulfils these criteria and allows the use of a continuous process [20].

Catalytically, bio-Pd has shown good activity in various reactions such as the dehalogenation of problematic polychlorinated biphenyls and pesticides [24–26] and the reduction of toxic Cr(VI) to Cr(III) [20,21,27–29], in hydrogenations [6,13] and in chemical syntheses (*e.g.* the Heck and Suzuki reactions [11,14]) as well as effective electrocatalysts for power generation in fuel cells [10,30].

In green chemistry applications various studies have suggested [29,31] that a loading of 5 wt% palladium on biomass is optimal. In early work Creamer et al. [13] evaluated 5 wt% bio-$Pd_{D.desulfuricans}$ in a standard reference reaction, the hydrogenation of itaconic acid, against a commercially available catalyst (5 wt% Pd/*C*), showing broadly similar activity of both catalysts. Subsequently it was reported [32] that 5 wt% bio-$Pd_{D.desulfuricans}$ was effective in catalysing a range of reactions in methanol, performing comparably to commercial catalyst in (e.g.) the conversion of 4-azidoaniline to 1, 4-phenylenediamine. In the hydrogenation of 3-nitrostyrene, the bio-Pd showed selectivity for the partly reduced (dehalogenated) product (1-ethyl-3-nitrobenzene-74%, 1-ethyl-3-aminobenzene-7%) whereas the commercial catalyst produced only the fully reduced product (1-ethyl-3-aminobenzene-73%). Similarly, in the case of 1-bromo-2-nitrobenzene, the bio-Pd was selective for the dehalogenated product, nitrobenzene, whereas the commercial catalyst produced aniline hydrobromide. These studies illustrate that bio-Pd-NPs may have a different pattern of activity as compared to commercial counterparts. In synthetic chemistry application of bio-Pd in the Suzuki reaction was shown [12] and the biomaterial was found to be comparably active or superior to colloidal Pd in the Heck reaction [11,14], giving a final conversion of 85% halide and initial rate of 0.17 mmol min^{-1} for the coupling of styrene and iodobenzene compared to a final conversion of 70% and initial rate of 0.15 mmol min^{-1} for a colloidal Pd catalyst under the same conditions.

Biomanufacturing has the potential to harness the infinite combinations of biochemistry (combining enzymatically-mediated synthesis and scaffolding functions) and hence potentially to exploit synthetic biology to make specific catalysts tailored for particular applications. The activity of 5 wt% mass Pd was comparable in hydrogenation of itaconic acid using examples of the two main types of bacterial cells (Gram negative: *D. desulfuricans* and Gram positive: *Bacillus sphaericus*) [13]; however a later study suggested that some Gram positive bacteria (*Micrococcus, Arthrobacter*) produced an inferior catalyst in the reduction of Cr(VI), while between related Gram negative bacteria the activity of the produced 'bio-Pd' was broadly similar [15]. Other work showed that in the dehalogenation of chlorinated aromatic compounds the activities of bio-$Pd_{D.desulfuricans}$ and bio-$Pd_{E.coli}$ were similar at 5 wt% Pd loading but at 25% mass loading the former was more active [29]. Conversely as a proton exchange membrane fuel cell catalyst 25% mass loading was required, with bio-Pd $_{D.desulfuricans}$ giving power output comparable to commercial catalyst [30].

In the selective hydrogenation of 2-pentyne, 5 wt% bio-$Pd_{D.desulfuricans}$ bio-catalyst was reported [6] to confer a higher selectivity towards *cis*-2-pentene than a commercial Pd on Al_2O_3 catalyst (5 wt% Pd), giving respective *cis*:*trans* ratios of 2.5 and 2.0 at a 2-pentyne conversion of 92%. 5 wt% bio-$Pd_{R.sphaeroides}$ was active in hydrogenation (24% of the *cis*-pentene but 60% of *trans*-pentene in 30 min from a 70.7:29.3 mixture) while 5 wt% bio-$Pd_{D.desulfuricans}$ removed 40% of 2-pentyne in 30 min but the activities of the two organisms were not compared directly [6]. Given that the activity and selectivity of bio-Pd in a particular reaction may be species-related, due to subtle differences in the local 'scaffolding' environment according to the precise cell surface composition and arrangement, the first objective of this study was to compare the activities of bio-$Pd_{D.desulfuricans}$ and bio-$Pd_{E.coli}$ as hydrogenation catalysts in comparison with commercial Pd/Al_2O_3 catalyst under similar conditions using two hydrogenation reactions of industrial importance. A rigorous comparison in a well understood chemical system is a key first step towards producing clean industrial catalysts via synthetic biology methods.

Other factors being equal, bio-Pd made by *E. coli* would be the catalyst of choice for commercial production for several reasons. H_2S (the product of dissimilatory sulfate reduction by *D. desulfuricans*), is a potent catalyst poison, requiring extensive washing of the catalyst prior to use. Growth of the obligately anaerobic *D. desulfuricans* is not readily scalable; it is generally killed by O_2 in air and H_2S is a highly toxic gaseous metabolic product, requiring strict safety procedures. Being facultatively anaerobic and producing no toxic by-products, *E. coli* can be pre-grown aerobically (to a ~10-fold higher biomass density than anaerobically) and then shifted to anaerobic conditions for upregulation of its hydrogenase activity (for reducing Pd(II) to Pd(0) [8,9]), reducing the cost of biomass production by up to 50 times. *E. coli* is also the standard 'workhorse' for molecular engineering, with resulting higher catalytic activity of the bio-Pd of an example engineered strain [33]. For large scale production of (*e.g.*) pharmaceuticals engineered strains of *E. coli* are widely used, with consequent disposal costs for the spent biomass. Hence, the second objective of this study was to evaluate the scope for using 'second life' cells of *E. coli* to make bio-Pd active in selective hydrogenation and to compare this material (bio-$Pd_{secondlife}$) with bio-Pd made by 'purpose-grown' cells.

Selective hydrogenations of vegetable oils, which are complex mixtures of fatty acids usually of different degrees of unsaturation, have significant applications in food and lubricant industries. The chemistry of the hydrogenation process is saturation of double bonds simultaneously involving geometric (*cis-trans*) and positional isomerisations [34–36]. The selective hydrogenation of vegetable oils aims to reduce the amount of polyenoic fatty acids (linolenic acid (*cis*-C18:3), linoleic acid (*cis*-C18:2)) to monoene (C18:1), while also reducing the formation of saturates (C18:0) or of *trans*-products (*trans*-C18:1) for food industry application and, in the lubricant industry, to improve the chemical stability, especially with regard to oxidation. Oleic acid (*cis*-C18:1), with a very low oxygen absorption rate [37,38], is industrially attractive, having the advantage of being stable in an oxygen atmosphere, while remaining liquid at low temperatures. In the food industry, the negative health effects of *trans*-fatty acids (TFA) (considered as being more detrimental than saturated fats [39]), are well-known. As a consequence, selectivity toward *cis*-fatty acids during vegetable oil hydrogenation is of sustained interest, with recent research emphasising the application of conventional noble metal catalysts. Nohair et al. [37] studied the selective hydrogenation of ethyl esters of sunflower oil (SOEE) (40 °C and H_2 pressure of 10 bar in ethanol) using silica-supported catalysts containing 1 wt% noble metals (Pd, Pt or

Ru), finding that the activity decreased in the order Pd > Pt > Ru. The effects of palladium precursors [40], the nature of supports [38,40], palladium particle size [38] and catalyst pore structure [41] were also investigated, as well as operating conditions [42–44] in slurry reactors. Despite substantial research on conventional palladium catalysts, catalytic selectivity toward *cis*-fatty acids remains a crucial problem in the hydrogenation process of vegetable oil. The *cis*-isomer is specifically sought in industrial hydrogenations such as olefin metathesis [45].

The third objective of this investigation was to evaluate the catalytic performance of conventional palladium catalyst (Pd/Al_2O_3) and the biomass-supported palladium NPs (bio-Pd) for selective hydrogenation of vegetable oil. The starting material, soybean oil, is a complex mixture of fatty acids, usually of different degrees of unsaturation (see Table 1). The chemistry of its hydrogenation is similar to, but more complicated than, 2-pentyne hydrogenation, being a saturation reaction of multiple carbon-carbon double bonds simultaneously involving geometric (*cis-trans*) and positional isomerisations. The reaction schemes of 2-pentyne and soybean oil hydrogenation, shown in Fig. 1a and b respectively, include the partial saturation of the carbon-carbon triple bond, the *cis-trans* isomerisation of the formed double bond and further saturation to form the alkane. Enhancing the production towards the desirable *cis*-monoene (*i.e. cis*-C18:1) remains a problematic issue in industry. The catalytic performance of the bio-Pd catalysts was compared against commercial Pd/Al_2O_3 catalyst in the partial hydrogenation of soybean oil, with the goal of improving the production of *cis*-isomer as compared to the commercial catalyst at a given degree of conversion.

2. Materials and methods

2.1. Chemicals

2-pentyne (>98%) and commercial soybean oil were purchased from Sigma-Aldrich (UK) and were used without further purification. The soybean oil contained mainly linolenic acid (*cis*-C18:3), linoleic acid (*cis*-C18:2), oleic acid (*cis*-C18:1), stearic acid (C18:0), and palmitic acid (C16:0) (Table 1). Conventional catalyst Pd/Al_2O_3 (Type 335) was supplied by Johnson Matthey, with an average size of 45 μm with distribution percentage reaching 50%.

2.2. Bio-catalyst manufacture

Bio-Pd was routinely prepared as 2 wt%, 5 wt% or as 25 wt% on bacteria where specified. Bio-$Pd_{D.desulfuricans}$ was prepared as described previously [6]. *Escherichia coli* MC4100 cultures were grown anaerobically at 37 °C in culture media (nutrient broth no. 2 (Oxoid) supplemented with sodium fumarate (0.4% wt/vol) and glycerol (0.5% vol/vol)) [9]. 'Second life' *E. coli* cells (strain IC007, a derivative of strain MC4100) were obtained from a primary process of hydrogen production (3 weeks) via the mixed acid fermentation [33]. The harvested cells were divided, half were bubbled with H_2 (30 min) and then H_2 was substituted for N_2, overnight (Method A). The other half was transferred to anaerobic respiratory medium (nutrient broth No 2 with 0.4% fumarate and 0.5% glycerol) overnight (30 °C: Method B). The cells were harvested by centrifugation and washed three times in degassed MOPS-NaOH buffer (20 mM, pH 7.0). The cell concentration, g(dry weight) L^{-1}, was estimated from optical density (OD_{600}) measurements by reference to a pre-determined OD_{600} to dry weight conversion, an OD_{600} of 1 corresponding to a biomass concentration of 0.482 g L^{-1} for *E. coli* [14].

Depending on the mass-percent loading required, a calculated volume of the resting cell suspension was transferred anaerobically into an appropriate volume of degassed (vacuum pump) 2 mM Pd(II) solution (Na_2PdCl_4). The cell/Pd(II) mixture was left to stand at 30 °C (30 min) to allow biosorption of Pd(II) complexes [46]. H_2 (electron donor) was sparged through the suspension (200 mL min^{-1}, 20 min) for reduction of Pd(II) [8]. Reduction of cell surface-bound Pd(II) to Pd(0) was monitored by observing the colour of the mixture (yellow to grey during H_2 sparging which corresponded to loss of Pd(II) from the solution by assay [47]). The Pd loaded cells were allowed to settle overnight under gravity then the black bio-Pd(0) precipitate was harvested by centrifugation, washed three times in distilled water and once in acetone. Washed bio-Pd(0) was then re-suspended in a small volume (~5 mL) of acetone, left to dry in air and finally finely ground to approximately 63 μm particle diameter (estimated by sieve) in an agate mortar.

2.3. Scanning and transmission electron microscopy (SAM and TEM) of Pd catalysts

For SEM dried samples of catalyst powder were mounted onto a microscope stub, coated with an ultrathin layer of electrically con-

Table 1
Fatty acid compositions and physical properties of untreated soybean oil.

Chemical properties			
Fatty acids	Trivial name	C-chain:double bonds[a]	Composition, wt%[b]
hexadecanoic acid	palmitic	C16:0	10.6–10.8
octadecanoic acid	stearic	C18:0	4.2–4.4
cis-9-octadecenoic acid	oleic	*cis*-C18:1	22.4 24.6
trans-9-octadecenoic acid	elaidic	*trans*-C18:1	<0.1
cis,*cis*-9,12-octadecadionic	linoleic	*cis*-C18:2	53.4–55.3
cis,*cis*,*cis*-9,12,15-octadecatrienoic acid	linolenic	*cis*-C18:3	6.8–7.4

Physical properties		
	Property	Reference
viscosity, μ, kg m^{-1} s^{-1}	$\log_{10}\mu = -3.073 + 46.6 \times 10^6 \times T^{-3}$	Haighton et al. [74]
density, ρ_L, kg m^{-3}	$\rho_L = 1108\text{-}0.65 \times T$	Bailey [75]
vapour pressure, p, MPa	$\log_{10} p^s = -1145 \times T^{-1} + 0.476$	Fillion and Morsi [66]

[a] C denotes carbon; the first number, *e.g.* 18, represents the total carbon number of the fatty acids; the second number, *e.g.* 3, represents the total number of double bonds.
[b] Weight percentage determined by GC, range from different batches of purchased oil.

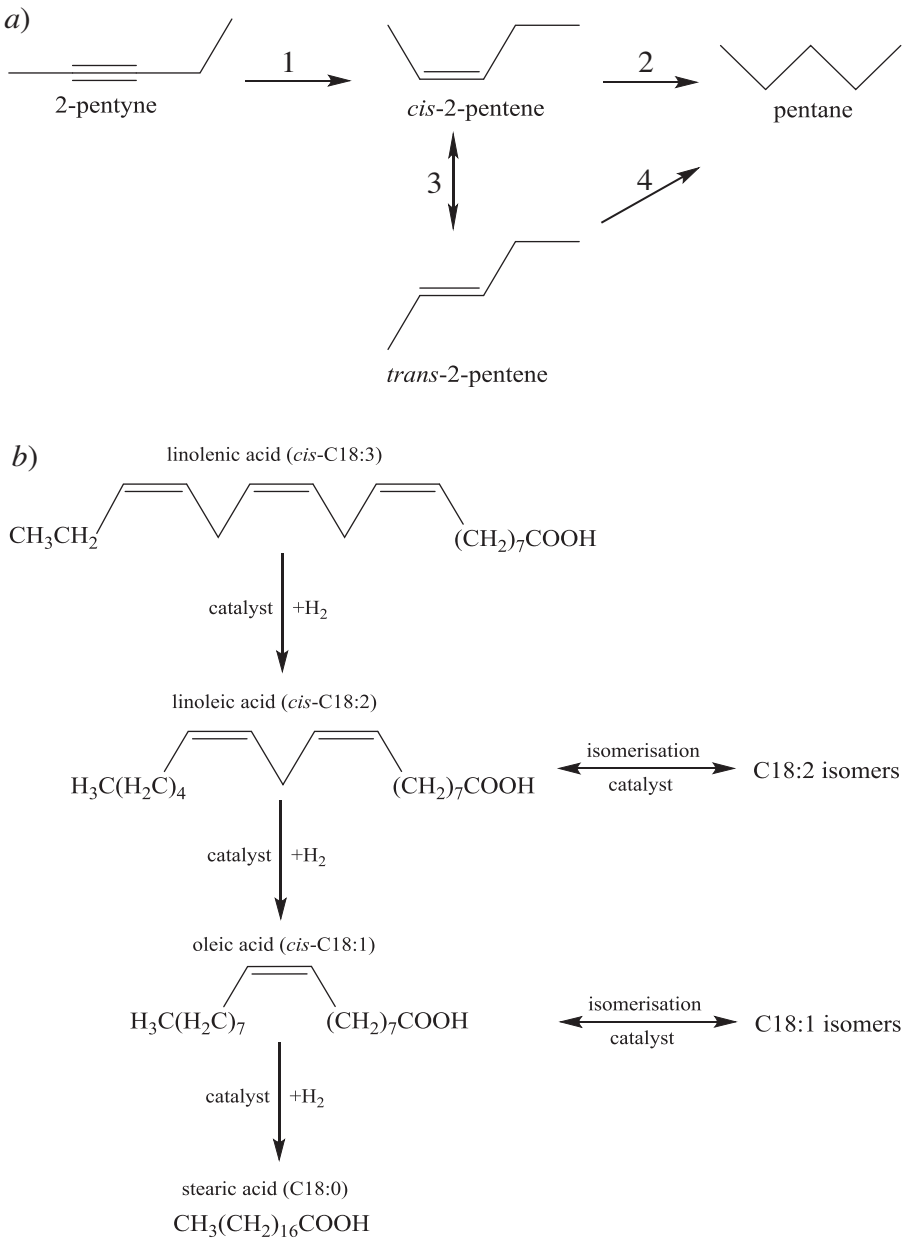

Fig. 1. a) The overall reaction scheme of 2-pentyne hydrogenation; b) Simplified soybean oil hydrogenation and isomerisation network in the presence of solid catalyst.

ducting material (graphite) by high-vacuum evaporation (Emscope SC 500 sputter coater), then examined on a Philips XL-30 Environmental SEM (vacuum mode) fitted with an Oxford Instruments Inca energy dispersive X-ray spectroscopy (EDS) system, operating at an accelerating voltage of 10 kV. A backscattering detector visualised the metallic NPs on the biomass and elemental analysis of the metallic NPs was determined by EDS. Detector controlling, data analysing and processing were performed using INCA software.

Catalysts were prepared for TEM as follows. For whole cells dried catalyst powder was dispersed in ultra-high purity water. A drop of the suspension was then evaporated on a holey carbon film supported by a 300 mesh copper TEM grid. For viewing cell structures a sectioning procedure used freshly harvested metal-loaded bacteria. These were rinsed twice with distilled water, fixed in 2.5% (wt/vol) glutaraldehyde, centrifuged, re-suspended in 1.5 mL of 0.1 M cacodylate buffer (pH 7) and stained in 1% osmium tetroxide in 0.1 M phosphate buffer, pH 7 (60 min). Cells were dehydrated using an ethanol series (70%, 90%, 100%, 100%, 100% dried ethanol, 15 min each) and washed twice in propylene oxide (15 min, 9500 g), embedded in epoxy resin and left to polymerise (24 h; 60 °C). Sections were cut from the resin block with a diamond knife (ultramicrotome), and placed onto a copper grid.

A JEOL 1200EX2 TEM (accelerating voltage of 80 kV) was used to view the specimens. TEM images were acquired in Gatan Digital Micrograph and processed using ImageJ software. For the measurement of the particle size distribution, at least 100 individual surface metal particles were examined for each catalyst.

2.4. X-ray powder diffraction analysis

X-ray powder diffraction patterns were acquired using an Equinox 3000 Powder X-Ray diffractometer. The catalyst powder was packed into the sample cup to the top. The analysis was conducted *via* monochromatic high-intensity CuKα radiation (λ' = 0.154056 nm). 'Match!' software was employed to process the data, and the powder pattern was compared to references in the

Table 2a
Parameters for different catalysts in this study.

	Hydrogenation conditions in Baskerville reactor	
Substrate	2-pentyne	soybean oil
Solvent	isopropanol	solvent-free
Catalyst	Pd/Al_2O_3	Pd/Al_2O_3
	Bio-$Pd_{D.desulfuricans}$[a]	Bio-$Pd_{D.desulfuricans}$
	Bio-$Pd_{E.coli}$	Bio-$Pd_{E.coli}$
Stirring speed (N, rpm)	1000	500–1200
Pressure (p, bar)	2, hydrogen	3–7, hydrogen
Temperature (T, °C)	40	100–150

[a] Not tested in this study; data taken from Bennett et al. [6].

Table 2b
GC columns and oven conditions for the analysis of different substrates in this study.

GC column, detector and oven conditions	2-pentyne hydrogenation	Soybean oil hydrogenation
GC column: capillary column	30 m γ-DEX™ 225	75 m SP™-2560
Carrier gas (helium) flow rate, mL min^{-1}	30.0	24.0
Injector temperature, °C	200	250
injection volume, μL	0.1	0.5
Detector temperature, °C	220	265
Temperature range	11	11
Oven equilibrium time	–	5.0 min at 200 °C
Oven isothermal temperature and time	40 °C for 10 min	–
Oven temperature ramp rate	–	4 °C min^{-1}
2nd isothermal temperature and time	–	240 °C for 15 min

Crystallography Open Database (COD). The nanoparticle size was calculated by application of the Scherrer equation.

2.5. Evaluation of catalytic activity

Reactions were conducted in a 500 mL high-pressure stainless steel autoclave reactor (Baskerville, Manchester, U.K.) in a semi-batch operation. Typically, the reactor was charged with a weighed mass of catalyst and a known volume of 2-pentyne in isopropanol (solvent) or soybean oil solvent-free (unless otherwise stated) substrate. For all the 2-pentyne hydrogenation experiments, the amount of the substrate used was 4 mL of 2-pentyne in 150 mL of isopropanol. The reactor was closed and purged with nitrogen three times to displace oxygen from the reactor headspace and liquid. The reactor was programmed to heat to the desired reaction temperature with stirring (~500 rpm or as otherwise stated). The reaction was initiated by substituting a hydrogen gas flow and maintained under H_2 at 2 bar pressure or as otherwise specified. Reactant gas (H_2) consumed was automatically replenished to maintain this set pressure *via* a controller. The reaction proceeded isothermally, during which liquid samples were taken periodically for analysis by gas chromatography (Tables 2a and 2b).

The palladium loadings in 2-pentyne and soybean oil were maintained at 0.375 mg(Pd) mL(2-pentyne)$^{-1}$ and 0.05 mg(Pd) mL(oil)$^{-1}$ respectively for each test. The catalyst weight, if of a variable Pd loading (*e.g.* 2 wt%, or 5 wt%), was adjusted in order to keep constant the weight of Pd between various experiments to be compared.

The catalytic activity of the Pd catalyst was initially evaluated by estimating the conversion of reactant, which is defined as the fraction of the reactant that has been consumed with respect to the original amount after the corresponding reaction time as follows:

$$\text{Reactant conversion (\%)} = ([\text{reactant}]_0 - [\text{reactant}]_t)/[\text{reactant}]_0 \times 100 \quad (1)$$

where $[\text{reactant}]_0$ and $[\text{reactant}]_t$ correspond to the concentrations at initial time (t = 0) and subsequent time (t) respectively.

The kinetics of 2-pentyne and soybean oil hydrogenations were analysed using the reaction rate equations derived based on a Langmuir-Hinshelwood type relationship. By taking into account the *cis-trans* isomerisation of the carbon-carbon double bond, which was considered following the well-known Horiuti-Polanyi mechanism [48], the overall reaction rates of the key components during the course of the hydrogenation reactions were derived. The model parameters were simultaneously estimated using a Solver function of MS Excel software, by minimising the sum of the squares of the difference between experimental and calculated concentration for each component. A constraint was imposed that the coefficients must be greater than or equal to zero.

3. Results and discussion

3.1. Characterisation of bio-Pd catalysts

The bio-catalyst material comprises black powder containing cells which are killed and permeabilised by the metallisation process and acetone washing; the dead bacteria act as a carbon-based support for metallic NPs, providing a similar function to conventional catalyst supports such as various forms of carbons, Al_2O_3 or TiO_2.

Initial studies compared the bio-$Pd_{D.desulfuricans}$ and bio-$Pd_{E.coli}$ using TEM (Fig. 2). Images were processed of nanoparticles at the cell surfaces using appropriate software ('Image J' [50]) with the aim to compare the average metal grain size for the bio-catalysts. Fig. 2 shows TEM images and the corresponding particle size distribution plots of 5 wt% bio-Pd catalysts. Details of cellular structure are not visible in the *D. desulfuricans* preparation (unstained with osmium: Fig. 2a), but this shows the discrete palladium NPs around the cell perimeter. A detailed EM analysis of bio-$Pd_{D.desulfuricans}$ was reported previously [50]. Examination of bio-$Pd_{E.coli}$ (Fig. 2c, circled) shows the presence of similar small intracellular NPs as described for *D.desulfuricans* [50]. For comparison the size calculations were made using only surface NPs including those associated with the inner membrane (Fig. 2f arrowed).

A TEM image of an ultra-thin section of native *E. coli* shows the double membrane structure evident in cells before metallisation as well as an absence of electron opaque material in the absence of added Pd. Cell structures are indistinct in the absence of osmium staining (Fig. 2e) The layers of the *E. coli* cell surface are denoted, following the direction of the arrow from the outer membrane (*o*), the inner (cytoplasmic) membrane (*i*), and the periplasmic space between these two membrane layers (width 20–50 nm). In contrast to the Pd-free cell section, the small discrete electron-opaque Pd(0) deposits (black dots indicated) were clearly observed, resolvable to individual particles. Most of the palladium NPs (arrowed; Fig. 2f) were held as discrete NPs beneath the outermost cell layers and bounded by the Gram-negative double membrane structure. The majority of NPs exhibited apparent monodispersity, although some larger clusters were observed in some cases (arrowed; Fig. 2c).

For each preparation at least 100 individual metal particles around the cell surface were examined; the corresponding mean grain sizes of the two bio-Pd catalysts are shown in Fig. 2b and d. By TEM, the palladium particle size on *D. desulfuricans* (5 wt%) was estimated to be 4.7 nm by measurement (range shown in Fig. 2b), which confirms the range of 2–5 nm reported by Creamer et al. [13]. The mean particle size of 5 wt% $Pd_{E. coli}$ was comparable by TEM at 4.31 nm (range shown in Fig. 2d). The nanoparticle size distribution on *E. coli* was narrower, with the majority of NPs within the size range 3–5 nm (Fig. 2b) while those on *D. desulfuricans* were more broadly distributed, with most between 3–7 nm (Fig. 2a).

By examination of the bio-$Pd_{D.desulfuricans}$ and bio-$Pd_{E.coli}$ (Fig. 2; Table 3) it was concluded that differences between them were small

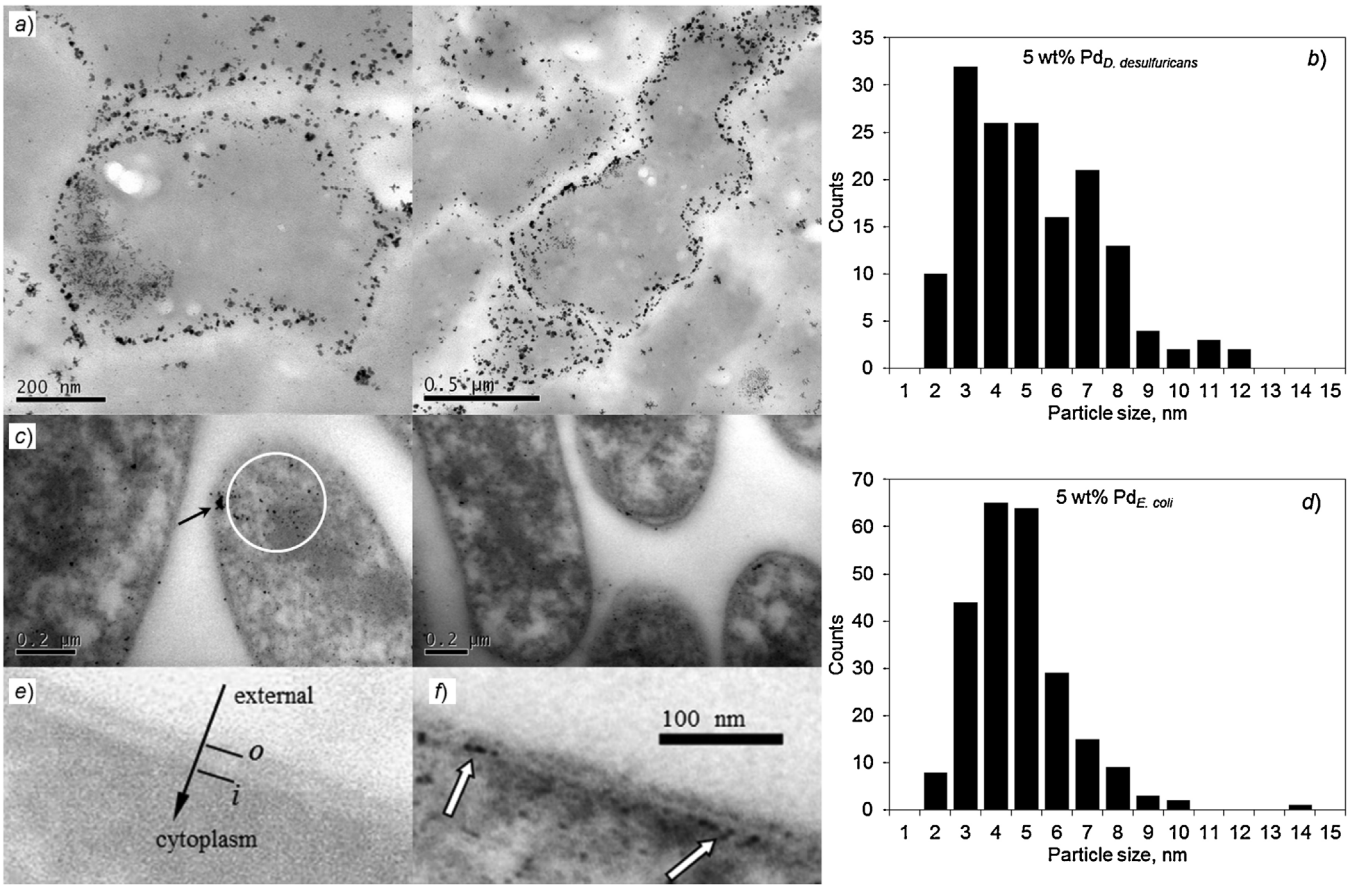

Fig. 2. TEM images of ultra-thin sections (unstained with osmium in a and e; stained in c and f) a: 5 wt% bio-$Pd_{D.desulfuricans}$ catalyst powder. Two images shown were used for the acquisition of particles representing two different areas from one single catalyst preparation; 155 surface particles were estimated with b) showing the particle size distribution (see text in Section 3.1). c) TEM images of ultra-thin sections made from two separate batches of freshly palladised 5 wt% bio-$Pd_{E.coli}$; note occurrence of small intracellular nanoparticles (circled). 240 surface particles were estimated (see text in Section 3.1) with the particle size distribution shown in d. e) An unstained cell section shows the cell surface layers o: outer membrane; i: inner membrane. f) A high resolution image of the cell surface region shows localisation of small NPs outward and inward facing on the inner membrane.

overall but the size distribution of the bio-$Pd_{E.coli}$ NPs was narrower than that of bio-$Pd_{D.desulfuricans}$, the latter having a larger proportion of NPs of greater than 5 nm (Fig. 2).

Typical SEM surface images of the dry powder of bio-$Pd_{E.coli}$ are shown in Fig. 3a. Individual bacteria are evident as rod-shaped cells of length 1–2 μm. In comparison, the conventional 5 wt% Pd/Al_2O_3 catalyst comprises spherical catalyst particles of ~20 μm (Fig. 3b). SEM examination of the cells cannot easily distinguish metal deposition on the bacteria. By detecting backscattered electrons (Fig. 3c) the presence of metal particles is clearly evidenced as bright dots, confirmed as Pd by EDS (Fig. 3d). In this case a higher Pd loading (25 wt%) was selected for the confirmation of Pd peaks from the EDS spectra, since EDS is relatively insensitive at low metal concentrations.

The X-ray powder patterns obtained from bulk preparations of bio-$Pd_{E.coli}$ with different palladium loadings (2 wt% Pd, 5 wt% Pd, and 25 wt% Pd: Fig. 3e) show an enhancement of peaks diagnostic of Pd (by comparison with the Crystallography Open Database: COD 96–900-8479) in the order from 2 wt% Pd, 5 wt% Pd to 25 wt% Pd. No defined peaks were visible at a loading of 2 wt% Pd, suggesting an amorphous material. Upon increasing the palladium loading to 5 wt%, broad peaks appeared in the XRD pattern becoming sharper at 25 wt%. The peak width from XRD patterns varies inversely with crystallite size. The crystallite sizes of the cell-bound Pd(0) of 5 wt% Pd and 25 wt% Pd on *E. coli* cells were estimated using Scherrer's equation [49] to be 4.12 nm and 28.74 nm. The former size is in good agreement with the average particle size determined by the TEM method (Fig. 2b and d) and with published data for bio-$Pd_{D.desulfuricans}$ (Table 3).

For bio-catalysts made on anaerobic Gram-negative bacteria, hydrogenases were shown to 'direct' the location of metal particles [9,10], supplying electrons from the splitting of hydrogen to promote reduction of Pd(II) to Pd(0) and acting as nucleation sites for the formation of Pd(0) NPs. Mikheenko et al. [10] investigating *D. fructosovorans,* which has four hydrogenases (two periplasmic and two bound within the inner membrane), found that removal by mutation of the major periplasmic hydrogenase resulted in relo-

Table 3
Comparison of bio-$Pd_{D.desulfuricans}$ and bio-$Pd_{E.coli}$. A summary of the catalyst characterisation data on different catalysts using different technologies.

Support	Metal loading	Metal particle size, nm		
	Pd, wt%	D_1[a]	D_2[b]	D_3[c]
E. coli				
	5.0	4.31	4.12	
	25.0	–	28.74	
D. desulfuricans				
	5.0	4.71	–	2–5*–3.1

*Creamer et al. [13].
#Bennett et al. [11].
[a] D_1: Average metal grain size estimated by TEM measurements and image analysis software Image J).
[b] D_2: Crystallite size estimated by XRD technique.
[c] D_3 Particle size value obtained from the literature.

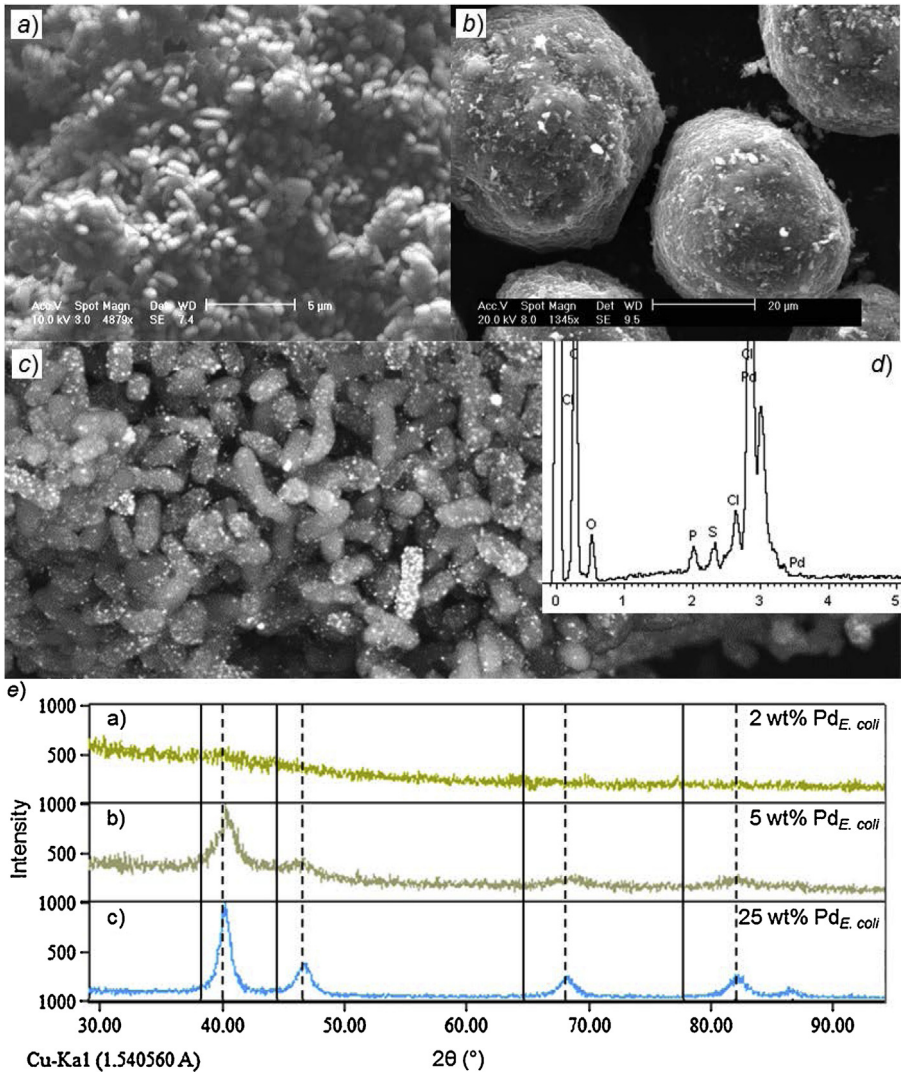

Fig. 3. SEM study of bio-Pd$_{E.coli}$. a) bio-catalyst powder at loading of 5 wt% Pd. Note rod-shaped cells of length 1 ~ 2 μm but catalyst NPs are not visible on the cells; b) SEM image of conventional 5 wt% Pd/Al_2O_3 catalyst; c) By loading the cells to 25 wt% with Pd and viewing using backscattered electrons (dried bio-Pd powder) nanoparticles are visible; d) Confirmation of NP identity as Pd using EDS; e) X ray powder diffraction analysis of bio-Pd$_{E.coli}$ at mass loadings of 2 wt% (top), 5 wt% (middle) and 25 wt% (bottom) Pd.

cation of the Pd(0) NPs from the periplasm to the inner cytoplasmic membrane. It also has been suggested that the polymeric nature of intertwined cell surface layers could offer support to the growing palladium NPs and hold them as stable entities [32] and the participation of cellular biochemical materials as 'abiotic' contributors to Pd(II) reduction has also been suggested [see 15]. However in the absence of all major hydrogenases the bio-Pd NPs formed on *E. coli* were large and were confined to the outermost cell surface [6], which suggests little abiotic reduction within the cell surface layers.

3.2. Comparison of bio-Pd$_{D.desulfuricans}$ and bio-Pd$_{E.coli}$ as catalysts in the hydrogenation of 2-pentyne

The above study indicates that, although the mean NP size is similar the bioPd$_{E.coli}$ material may offer a more uniform NP size overall and slightly smaller NP size. The two types of bio-Pd were compared with respect to the rate of hydrogenation of 2-pentyne (Table 4) with reference to the hydrogenation by Pd/Al_2O_3 under the same conditions. For bio-Pd$_{D.desulfuricans}$ the conversion rate was approx. 3.5-fold slower than for the commercial Pd on Al_2O_3 catalyst at a slow stirring speed, but was increased by ~6-fold on increasing the stirring speed to 1100 rpm [6]. In the present study using a stirring speed of 1000 rpm (increasing the stirrer speed above 800 rpm did not enhance the reaction rate: see 3.4.1) the 2-pentyne consumption rate using 5 wt% bio-Pd$_{E.coli}$ was 3-fold higher than by using 5 wt% Pd/Al_2O_3 and for bio-Pd$_{D.desulfuricans}$ by ~30% (Table 4). Since *E. coli* is the better organism for future development (see Introduction) further studies focused on the *E. coli* material.

3.3. Comparison of bio-Pd$_{E.coli}$ and Pd/Al_2O_3 as catalysts in the hydrogenation of 2-pentyne

Since 2 wt% bio-Pd$_{E.coli}$ gave very small NPs as shown by XRD analysis (above) it might be expected that they would have good catalytic activity, as shown previously where a good hydrogenation catalyst was obtained by using 2 wt% Pd on *D. desulfuricans* [13]. In this work, the reaction conditions were optimal as determined by Bennett et al. [6] (T = 40 °C, pH_2 = 2 bar, and stirring speed of 1000 rpm; 4 mL of 2-pentyne in 150 mL of isopropanol). Isopropanol was selected as a solvent as it gives a respectable rate of reaction and a high selectivity towards the alkene. The effect of the solvent was previously investigated by Bennett et al. [6],

who studied the same reaction using a non-polar solvent heptane, a polar solvent isopropanol and a 1:1 mixture of the two. It was found that the rate for the reaction run in heptane was 1.85 mol s^{-1} $kgPd^{-1}$ compared with 5.63 mol s^{-1} $kgPd^{-1}$ for the reaction carried out in isopropanol, although the rates and selectivity were quite dependent upon catalyst type and loading. The solvent choice affects the alkyne and hydrogen solubility, dispersion or agglomeration of catalyst and rate of diffusion of the reactants into the catalyst pores, as previously investigated [6]. Additionally solvents can sometimes act as hydrogen donors, although previous unpublished experiments using deuterated water as a solvent did not show any evidence of the water participating in the reaction. Typical concentration profiles for 2-pentyne hydrogenation using 2 wt% bio-$Pd_{E.coli}$ are shown in Fig. 4a. Complete hydrogenation was achieved within 40 mins. *Cis*-2-pentene was the major product during the initial 30 mins, suggesting preferential *syn*-addition of hydrogen onto the triple bond (C≡C) (step 1 in Fig. 1a). The other two identified products, *trans*-2-pentene and pentane, were formed slowly at approximately equal rates. Bio-$Pd_{E.coli}$ at 2 wt% and 5 wt% loading was compared with Pd/Al_2O_3 as shown in Fig. 4b. Specific rates are shown in Table 4. Whereas at 5 wt% loading of Al_2O_3 and 2 wt% loading of bio-$Pd_{E.coli}$ the activities were comparable (Table 4) the bio-Pd was better than Al_2O_3 at 5 wt% loading, with 50% conversion reached after 7 mins as compared to 10 mins by the commercial counterpart (Fig. 4b) and a comparison of the initial rates confirmed that 5 wt% bio-$Pd_{E.coli}$ gave a faster initial reaction rate (by ~30%) than the 2 wt% Pd/Al_2O_3 (Table 4).

Whereas a previous study using bio-$Pd_{D.desulfuricans}$ reported a maximum concentration of *cis* 2-pentene of about 50% of the mixture after 30 mins using 5 wt% bio-Pd [6] the concentration of *cis*-2-pentene produced by 2 wt% bio-$Pd_{E.coli}$ reached $18.1 \pm 0.4 \times 10^{-2}$ mol L^{-1} (~66.7 wt% of the mixture) at 20–30 min (Fig. 4a), and began to fall at >90% of 2-pentyne conversion, concurrently with a continuing increase in both the *trans*-2-pentene and pentane components (Fig. 4a). This implies that the reaction path is the hydrogenation of 2-pentyne to *cis*-2-pentene followed by its deposition and re-adsorption for further hydrogenation to pentane or *cis-trans* isomerisation to *trans*-2-pentene.

The adsorption of alkyne on the palladium surface has been suggested to be stronger than that of the corresponding alkene [51–55] and thus could prevent the re-adsorption of the product alkene [45,56]. Hence, *cis*-2-pentene is able to compete for the metal active sites only when most of the 2-pentyne is consumed from the solution, to be further hydrogenated to pentane or converted to its *trans*-isomer. As a consequence, *cis*-2-pentene was not consumed in the presence of more than 10% residual 2-pentyne (0–30 mins in Fig. 4a), but underwent hydrogenation and isomerisation on depletion of the latter. The mole balance of the liquid substances was conserved during the course of the reaction. Analysis of molecular interactions was outside the scope of this study but the higher proportion of NPs that are larger (between 6–14 nm) in the case of bio-$Pd_{Ddesulfuricans}$ (Fig. 2b) means that these will have proportionally less atoms at 'edges' as compared to the more numerous smaller NPs of bio-$Pd_{E.coli}$ and, assuming that the molecular shape of the *cis*-isomer is a better 'fit' to the crystal edges this small

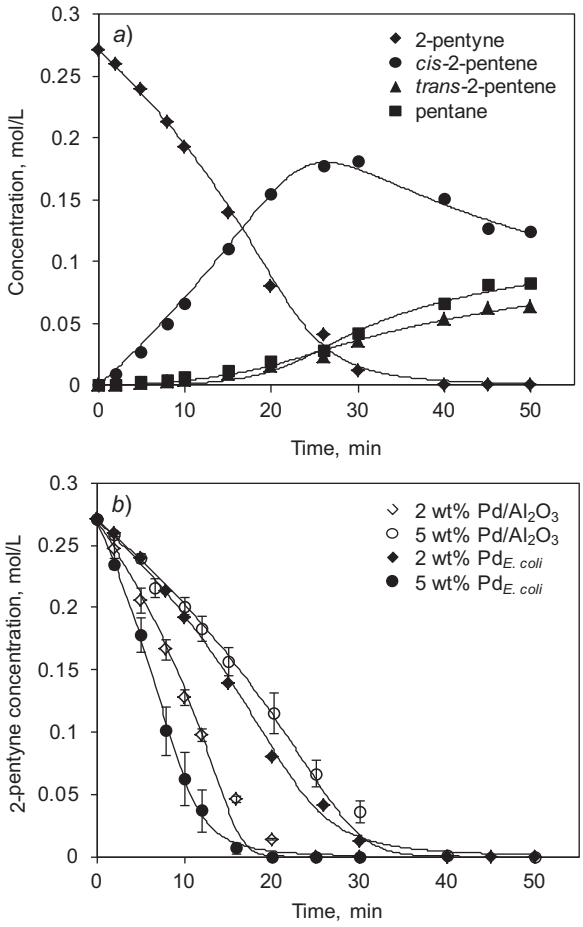

Fig. 4. a) Concentration profiles as the function of reaction time in 2-pentyne hydrogenation using a 2 wt% $Pd_{E.coli}$ catalyst. Reaction conditions were: 75 mg of 2 wt% $Pd_{E.coli}$, 4 mL of 2-pentyne, 150 mL of isopropanol (solvent), $T = 40\,^{\circ}C$, $pH_2 = 2$ bar, $N = 1000$ rpm. Symbols are experimental data points averaged from two experiments with a reproducibility of within 10%. Compounds are: ♦ : 2-pentyne; ●: *cis*-2-pentene; ▲: *trans*-2-pentene and ■: pentane. b) 2-pentyne concentration profiles versus reaction time over Pd/Al_2O_3 and bio-$Pd_{E.coli}$ catalysts. Reaction conditions were: 30 mg of 5 wt% Pd (or 75 mg if 2 wt% Pd), 4 mL of 2-pentyne, 150 mL of isopropanol (solvent), $T = 40\,^{\circ}C$; $pH_2 = 2$ bar, $N = 1000$ rpm. Where error bars are shown these were calculated as mean ± standard error of the mean from at least three experiments. Where no error bars are shown (2 wt% $Pd_{E.coli}$) the data were averaged from two experiments with a reproducibility of within 10%. Catalysts were: ◊: 2 wt% Pd/Al_2O_3; ○: 5 wt% Pd/Al_2O_3; ♦: 2 wt% bio-$Pd_{E.coli}$; ●: 5 wt% bio-$Pd_{E.coli}$. Lines shown represent the kinetic model (fitted to experimental data; see text in 3.3).

Table 4
Catalytic activities of bio-$Pd_{D.desulfuricans}$, bio-$Pd_{E.coli}$ and Pd/Al_2O_3 catalysts in hydrogenation of 2-pentyne.

	Rate of 2-pentyne conversion[a], mol 2-pentyne min^{-1} mg $(Pd)^{-1}$	Product concentration, $\times 10^{-2}$ mol L^{-1}		
		cis-2-pentene	*trans*-2-pentene	pentane
2 wt% Pd/Al_2O_3	1.34×10^{-3}	7.34 ± 0.53	10.29 ± 0.60	9.44 ± 0.48
5 wt% Pd/Al_2O_3	0.63×10^{-3}	6.52 ± 0.46	9.62 ± 0.38	10.94 ± 0.79
2 wt% $Pd_{E.coli}$	0.64×10^{-3}	15.11	5.36	6.61
5 wt% $Pd_{E.coli}$	1.90×10^{-3}	10.09 ± 0.52	6.20 ± 0.54	9.96 ± 0.64
5 wt% $Pd_{D.desulfuricans}$[b]	1.33×10^{-3}	–	–	–

[a] Rate was determined at 5 min reaction time. Product is shown at 100% 2-pentyne conversion. Reaction conditions were 30 mg of 5 wt% Pd (or 75 mg if 2 wt% Pd) catalyst, 4 mL of 2-pentyne, 150 mL of isopropanol (solvent), $T = 40\,^{\circ}C$, $pH_2 = 2$ bar, $N = 1000$ rpm.
[b] Data from earlier studies [6] and normalised against 5 wt% Al_2O_3, reaction conditions were the same as above apart from $N = 1100$ rpm. Data are means ± SEM for three experiments or the mean from two experiments (where no SEM is shown; agreement was within 10%).

Table 5
Values of fitted parameters for 2-pentyne hydrogenation.

Catalyst	Rate constant $\times 10^{-3}$ mol g^{-1} s^{-1}				Adsorption coefficient $\times 10^{-3}$ m^3 mol^{-1}		
	k'_{Py}	$k_{cis\text{-}trans}$	$k_{trans\text{-}cis}$	k'_{Pe}	K_{Py}	K_{Pe}	K_{Pa}
2 wt% $Pd_{E.coli}$	22.3	0.2	0	2.9	28.48	12.20	0.002

k'_{Py}, k'_{Pe}: hydrogenation rate constants; $k_{cis\text{-}trans}$, $k_{trans\text{-}cis}$: *cis-trans* isomerisation rate constants. K_i: adsorption coefficient of *i*, m^3.mol^{-1}. Py, *cis*-Pe, *trans*-Pe, and Pa denote 2-pentyne, *cis*-2-pentene, *trans*-2-pentene, and pentane correspondingly.

difference between the two types of bio-Pd may be sufficient to account for the superiority of the bio-$Pd_{E.coli}$ if not entirely due to the respective surface areas of the bio-$Pd_{E.coli}$ having a larger number of smaller particles.

Table 4 also compares the product distribution at 100% 2-pentyne conversion using the Al_2O_3 and bio-$Pd_{E.coli}$ catalysts. At an equal Pd loading into the reactor, the latter selectively produced a significantly higher amount of *cis*-2-pentene and a lower yield of the unwanted *trans*-isomer than the Al_2O_3-supported counterpart, with a higher concentration of *cis*-2-pentene by 2 wt% bio-Pd (Table 4) offsetting the lower reaction rate (Fig. 4b). The better selectivity towards *cis*-2-pentene over bio-$Pd_{E.coli}$ can be attributed to a smaller average size of Pd particles as compared to Pd/Al_2O_3 at an equivalent Pd loading, *e.g.* 4.31 nm for 5 wt% bio-$Pd_{E.coli}$ and 12.77 nm [57] for 5 wt% Pd/Al_2O_3. The NP size at 2 wt% Pd was not calculated since the Pd was largely amorphous as shown by XRD (Fig. 3e).

The fitted lines in Fig. 4b were a good match to the experimental data points. Table 5 shows the predicted values of the kinetic and adsorption parameters at loadings of 2 wt% Pd showing that the reaction for bio-$Pd_{E.coli}$ obeys 'classical' reaction chemistry as described for inorganic supported catalysts. Hydrogenation rate constants estimated by the model indicate a 7.6-fold faster hydrogenation of the carbon-carbon triple bond (C≡C) than that of the carbon-carbon double bond (C=C), which were 22.3×10^{-3} mol g^{-1} s^{-1} and 2.9×10^{-3} mol g^{-1} s^{-1} respectively. Values of *cis-trans* isomerisation rate constants ($k_{cis\text{-}trans}$ and $k_{trans\text{-}cis}$) were predicted to be lower than those of hydrogenation rate constants (k'_{Py} and k'_{Pe}), suggesting a lower level of isomerisation than hydrogenation. A stronger adsorption of 2-pentyne than that of 2-pentene, and a very weak adsorption of pentane on the active site are revealed by the model-predicted values of adsorption coefficients ($K_{Py} > K_{Pe} >> K_{Pa}$). Very few values of the rate constant and adsorption coefficient of 2-pentyne in a similar hydrogenation process are reported in the literature for the purpose of comparison. However, it is noteworthy that in the hydrogenation of 2-butyne-1,4-diol in isopropanol over bio-$Pd_{A.oxydans}$, Wood et al. [58] reported adsorption coefficients of 2-butyne-1,4-diol and 2-butene-1,4-diol of 31.28 m^3 mol^{-1} and 0.00 m^3 mol^{-1}. In another study of 2-methyl-3-butyn-2-ol hydrogenation over a $Pd/CaCO_3$ catalyst (solvent free) by Bruehwiler et al. [59], the estimated adsorption coefficients of 2-methyl-3-butyn-2-ol and 2-methyl-3-buten-2-ol were small (10^{-3} m^3 mol^{-1} and 10^{-5} m^3 mol^{-1} respectively). Although this cannot be compared directly with Table 5 due to the use of different substrates, catalysts and reaction conditions, it is evident that the adsorption of alkyne on a palladium surface is stronger than that of alkene.

One of the key objectives of this study is to compare the catalytic performance of bio-$Pd_{E.coli}$ in 2-pentyne hydrogenation with that of the conventional catalyst Pd/Al_2O_3. From Fig. 4b it is concluded that under the same reaction conditions, the 2-pentyne consumption rates decreased in the order of catalysts: 5 wt% $Pd_{E.coli}$ > 2 wt% Pd/Al_2O_3 > 2 wt% $Pd_{E.coli}$ close to 5 wt% Pd/Al_2O_3. It is assumed that the higher metal loading onto Al_2O_3 is not realised in terms of an increased Pd surface area whereas the patterning afforded by the bio-support can retain individual NPs without coalescence or aggregation. Notably, increasing the Pd loading from 2 wt% to 5 wt% upon Al_2O_3 decreased the catalytic activity whereas the converse was true with bio-$Pd_{E.coli}$. For the conventional Pd/Al_2O_3 catalyst, it is suggested that a lower Pd loading leads to a higher metal dispersion [60] with Pd particles possessing smaller size and larger surface area per unit mass of metal. In confirmation the 2 wt% Pd/Al_2O_3 and 5 wt% Pd/Al_2O_3 catalysts examined by CO pulse chemisorption analysis, revealed metallic surface areas of 57.85 m^2 g(metal)$^{-1}$ and 39.32 m^2 g(metal)$^{-1}$ respectively [57]. However CO chemisorption tests using bio-Pd were unsuccessful, possibly attributable to absorption of CO by the residual biomass component [57].

At the same Pd loading in each test 2 wt% Pd/Al_2O_3 provided the larger surface area, allowing a faster 2-pentyne conversion. The converse being true, *i.e.* 5 wt% bio-$Pd_{E.coli}$ giving the higher reaction rate, was attributed to Pd particle seeds being localised and patterned by the distribution of hydrogenases and their biochemical environment [9,10] to maintain NP stability at the increased surface area per NP without agglomeration; with increased metal loading the size, and not the number, of bio-NPs increases [57]. The relative contributions of the cell surface and intracellular NPs to the overall catalytic activity were not determined.

We conclude that in 2-pentyne hydrogenation the dual objectives of higher reaction rates and a lower yield of *trans*-pentene are met by using bio-$Pd_{E.coli}$ catalyst. Note also that commercial Pd/Al_2O_3 catalyst is the product of extensive prior industrial optimisation whereas bio-$Pd_{E.coli}$ was used 'as made' without any further development beyond the studies reported here. Based on this preliminary comparison, the more complex hydrogenation of soybean oil was investigated to assess whether the bio-$Pd_{E.coli}$ catalyst could be substituted for existing commercial material and to compare the activity of the former with bio-$Pd_{D.desulfuricans}$.

3.4. Hydrogenation of soybean oil

3.4.1. Conventional catalyst 5 wt% Pd/Al_2O_3

Fig. 5a shows a typical time course of fatty acid concentration profiles using 5 wt% Pd/Al_2O_3 under 5 bar of H_2 at 125 °C with a stirring speed of 800 rpm, following preliminary optimisation tests (supplementary information; Figs. S1 and S2). At the reaction onset, it is likely that the catalyst surface is saturated with the *cis*-C18:3 and *cis*-C18:2 components due to the strong multi-site adsorption *via* multiple C=C double bonds and the C=O bond of carbonyl groups [61]. Fig. 5a shows that the initial *cis*-C18:3 (~0.23 mol L^{-1}) was depleted within 1.5 h. The other major reactant *cis*-C18:2 (~1.77 mol L^{-1} initially) showed a conversion of 96.80 ± 1.31% after 2 h, with a residual mass percent of 1.74 ± 0.41 wt%.

Product formation during the reaction can be divided into 3 stages as shown in Fig. 5a. (i) Between 0–1 h both *cis*-C18:1 and *trans*-C18:1 were formed, indicating hydrogenation and isomerisation taking place simultaneously, as indicated by mirroring profiles, with the *cis*- and *trans*- isomers becoming equimolar after 1.5 h. According to the Horiuti-Polanyi mechanism [48], the half-hydrogenated intermediate is firstly formed on the catalyst surface, and the free rotation of the half-hydrogenated intermediate followed by hydrogen abstraction and desorption of the olefin results in *cis-trans* isomerisation. Hence, before the newly formed *cis*-C18:1 is desorbed from the active site, it is converted further to the

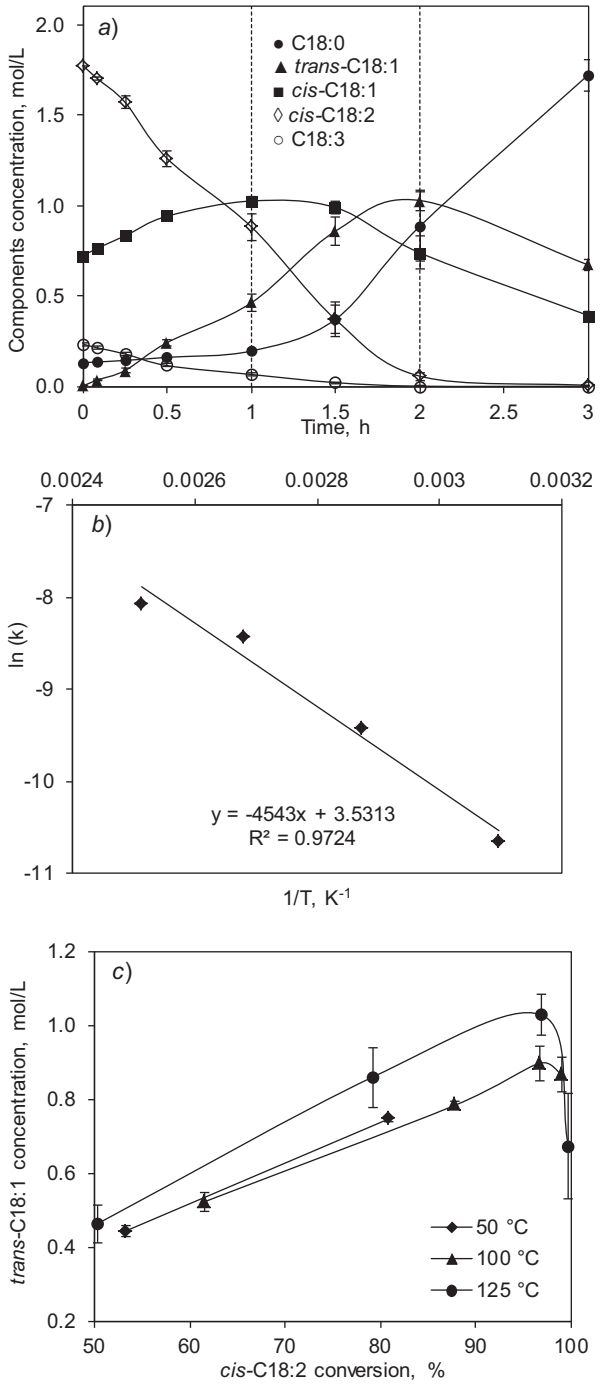

Fig. 5. Hydrogenation of soybean oil by Pd/Al_2O_3 catalyst. a) Product evolution with time. Reaction conditions were: 150 mg of 5 wt% Pd/Al_2O_3, 150 mL of soybean oil (solvent free), $T = 125\,^{\circ}C$, $pH_2 = 5$ bar, Stirring speed = 800 rpm. Vertical dashed lines at time of 1 h and 2 h divide the profile into 3 time intervals (see text in 3.4.1). ●: C18:0;▲: *trans*-C18:1; ■: *cis*-C18:1; ◊: *cis*-C18:2; ○: C18:3. b) Arrhenius plot of ln(k) versus 1/T showing temperature dependence of soybean oil hydrogenation over 5 wt% Pd/Al_2O_3 catalyst. Reaction conditions were as a) ($R^2 = 0.9724$) c) Formation of *trans*-C18:1 versus *cis*-C18:2 conversion in soybean oil hydrogenation using 5 wt% Pd/Al_2O_3 under different reaction temperatures (°C): ♦, 50; ▲, 100; ●, 125. Reaction conditions were as above).

higher thermochemically stable *trans*-C18:1 due to steric hindrance [62]. (ii) Between 1–2 h the concentration of *cis*-C18:1 decreased, mirroring *trans*-C18:1 product formation and with onset of C18:0 production after 1.5 h. A decrease of the polyenic fatty acid concentration (after 2 h a conversion of 100% was observed for *cis*-C18:3 and 96.8 ± 1.3% for *cis*-C18:2) could have vacated some of the catalyst active sites and thus allowed access for *cis*-C18:1 adsorption onto the catalyst surface, leading to the successive hydrogenation of *cis*-C18:1 giving C18:0 but also isomerisation to *trans*-C18:1, which increased between 1 and 2 h, indicating acceleration of the *cis-trans* isomerisation of *cis*-C18:1 during the consumption of *cis*-C18:2. (iii) Between 2–3 h both *cis*-C18:1 and *trans*-C18:1 decreased as a result of their hydrogenation to saturated C18:0, with only C18:0 accumulating, to a concentration of 1.7 ± 0.3 mol L^{-1} (~53.4 wt% of the mixture) after 3 h reaction time. From the above observations, the reaction path was suggested as the stepwise hydrogenation of polyenoic fatty acids (C18:3 and C18:2) to monoenoic fatty acid (C18:1) followed by deposition and re-adsorption for monoene (C18:1) and further hydrogenation to saturated fatty acid (C18:0), while the *cis-trans* isomerisation occurs as a parallel reaction of the unsaturated components. The mole balance of the liquid substances was conserved during the course of the reaction.

This hydrogenation, a typical multiphase catalytic process involving hydrogen (gas), soybean oil (liquid) and catalyst (solid), may suffer from hydrodynamic resistances and transport limitations attributable to a low solubility of hydrogen in the oil and the long carbon chains of reactant molecules in the liquid phase. For reactions under identical temperature and hydrogen pressure, hydrogen mass transfer rate in the gas-liquid interface is mainly determined by the volumetric liquid-side mass transfer coefficient k_La of hydrogen. Agitation speed plays an important role on k_La for a specific type of reaction in a given reactor configuration [63,64].

The initial reaction rates (over 30 min) were dependent on the agitation speed within the range up to ~800 rpm, above which the initial rates of both *cis*-C18:3 and *cis*-C18:2 conversion were independent of the stirring speed (not shown), implying the contribution of a higher volumetric gas-liquid mass-transfer coefficient k_La (s) of hydrogen, as suggested by Fernández et al. [64]. More specifically, the liquid-side mass-transfer coefficient k_L (m s^{-1}) is affected since increasing mixing speed increases the turbulence and surface renewal rate at the gas-liquid surface while decreasing the liquid film thickness, correspondingly increasing k_L [65,66]. Also the volumetric gas-liquid interfacial area a (m) could increase since a higher mixing speed introduces more gas into the slurry and breaks large gas bubbles into several small ones with larger specific surface area [65,67].

With respect to the effect of stirring speed on the product distribution pronounced effects were seen only at high *cis*-C18:2 conversion (> 70%) (supplementary information, Fig. S1); the stirring speed affected marginally the formation of the *trans*-C18 and C18:0. At slow speeds the lower hydrogen availability on the catalyst surface may increase the possibility of *cis-trans* isomerisation, as well as also promoting the transfer of product away from the catalyst surface. Since under agitation conditions of above 800 rpm, the gas-liquid mass transfer resistance was negligible this stirring speed was adopted.

Increasing the pressure to enhance the hydrogen dissolution would also increase the reaction rate and conversion. Pressures from 2 to 5 bar H_2 gave a nonlinear dependence of rate on H_2 pressure, indicating a fractional order-dependence with respect to H_2. Inconsistent findings are reported in the literature in terms of the hydrogen reaction order, *e.g.* a reaction order in hydrogen varying from 0.24 at 413 K to 0.54 at 473 K in rapeseed oil hydrogenation was reported by Bern et al. [68]; a half-order with respect to hydrogen was interpreted in the hydrogenation of butynediol in a batch slurry reaction by Chaudhari [69], while the hydrogen reaction order was proposed to be zero in a report of the partial hydrogenation of rapeseed oil in the presence of a supported palladium catalyst by Santacesaria et al. [70]. In this study, the observations of the effects of catalyst amount and hydrogen pressure on soybean oil hydrogenation over 5 wt% Pd/Al_2O_3 suggested that a fractional order with regard to the hydrogen concentration may be assumed.

However further tests would require to confirm the hydrogen reaction order.

The influence of hydrogen pressure on the product formation was also evaluated (supplementary information, Fig. S2) with a slightly higher amount of *trans*-isomer produced at 3 bar, with much less at 5 and 7 bar, suggesting that a low concentration of dissolved H_2 in the bulk liquid at low operating pressure promoted isomerisation on the catalyst surface, in preference to hydrogenation. A lower availability of H_2 also gave a lower production of saturated fatty acid (C18:0) at 3 bar H_2 (supplementary information, Fig. S2b). It appears that a low hydrogen concentration favours the *cis-trans* isomerisation. However it has been suggested that hydrogen is needed in isomerisation, which stops in its absence [71–73]. In the selective hydrogenation of fatty acid methyl esters of sunflower oil, Pérez-Cadenas et al. [71] found the isomerisation rate was weakly dependent on the hydrogen pressure although hydrogen was not consumed. The effect of hydrogen concentration on the reversible *cis-trans* formation in soybean oil hydrogenation was reported to give different hydrogen orders, 0.88 ± 0.01 for the *cis*-isomer to react (forward) and 1.56 ± 0.03 for the *trans*-isomer to react (backward) respectively [72]. Dijkstra [73], reporting on the isomerisation of the mono-unsaturated fatty acid suggested a half an order isomerisation in hydrogen. From supplementary information (Fig. S2) 5 bar of hydrogen pressure was chosen as a compromise between achieving an acceptable reaction rate and less formation of C18:0 for studies to compare Pd/Al_2O_3 (Fig. 5a) and bio-Pd (below).

In order to obtain the activation energy a series of reactions (as in Fig. 5a) was carried out at temperatures ranging from 50 °C, 75 °C, 100 °C to 125 °C. The temperature dependence of the reaction rate constants obeys the Arrhenius-type equation as:

$$\mathrm{Ln}(k) = \ln(A) - [(E_a/R)(1/T)] \quad (2)$$

where k = reaction rate coefficient ($\mathrm{mol\,m^{-3}\,s^{-1}}$), A = pre-exponential factor, E_a = activation energy ($\mathrm{kJ\,mol^{-1}}$), R = gas constant ($8.314\,\mathrm{J\,K^{-1}\,mol^{-1}}$), and T = absolute temperature (K).

Fig. 5b shows the resulting Arrhenius plot for soybean oil hydrogenation over 5 wt% Pd/Al_2O_3, with an activation energy obtained as $37.8\,\mathrm{kJ\,mol^{-1}}$. This is half of the activation energy ($75.5\,\mathrm{kJ\,mol^{-1}}$) reported by Fillion et al. [72] for soybean oil hydrogenation over a Ni/Al_2O_3 catalyst, confirming the superiority of Pd. Accordingly, the present value of activation energy is in close agreement with those in the work by Belkacemi and Hamoudi [43]. Their study reports [43] that within the experimental errors Pd-catalyst hydrogenates vegetable oils with quasi-similar activation energy, giving $38.6\,\mathrm{kJ\,mol^{-1}}$ and $40.1\,\mathrm{kJ\,mol^{-1}}$ in the hydrogenation of sunflower oil and canola oil correspondingly. The slight variation can be attributed to the different composition contents in vegetable oils, i.e. due to the higher content of stable and less reactive monounsaturated fatty acids (*cis*-C18:1, ~64% in canola oil and ~19% in sunflower oil [75]), canola oil was less reactive than sunflower oil.

With respect to the effect of temperature on product formation, Fig. 5c shows that a higher temperature slightly enhanced the formation of fatty acid *trans*-isomers at *cis*-C18:2 conversion >50%. Deliy et al. [61] suggested this effect was related to a reduction of concentration of hydride modes on the catalyst surface that led to an increased contribution of isomerisation.

3.4.2. Comparison of bio-$Pd_{E.coli}$ with Pd/Al_2O_3 catalyst

To compare the catalytic performance of the bio-$Pd_{E.coli}$ with that of Pd/Al_2O_3, the reactions were conducted with identical loadings of 0.05 mg(Pd) mL(oil)$^{-1}$ under optimised conditions as shown in Fig. 6a. A much slower reaction rate was observed for bio-$Pd_{E.coli}$ (Fig. 6a) as compared to the 5 wt% Pd/Al_2O_3 catalyst (Fig. 5a); here > 5 h was required for 50% conversion as compared to ~1 h for the commercial catalyst. After 5 h a residual *cis*-C18:2 concentration of $0.97 \pm 0.1\,\mathrm{mol\,L^{-1}}$ was obtained (conversion of $45.52 \pm 5.61\%$: Fig. 6a). The concentration of *cis*-C18:1 increased in parallel to the loss of *cis*-C18:2. Very little *trans*-C18:1 and C-18:0 were formed by the bio-$Pd_{E.coli}$ catalyst (Fig. 6a). Comparing the two catalysts (Fig. 6b) at the 5 h reaction time over 5 wt% $Pd_{E.coli}$, (~45% conversion) *cis*-C18:1 production accumulated to the highest con-

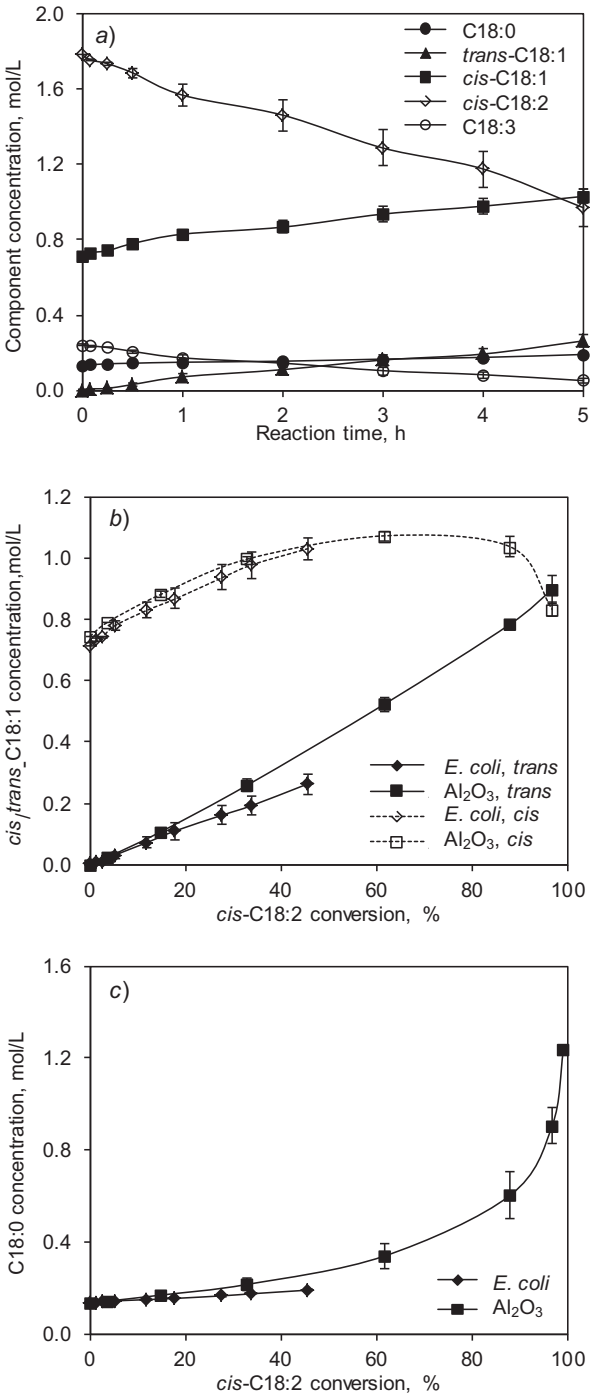

Fig. 6. Hydrogenation of soybean oil by bio-$Pd_{E.coli}$ a) Concentration profiles as the function of reaction time in soybean oil hydrogenation using 5 wt% $Pd_{E.coli}$. Reaction conditions were: 150 mg of 5 wt% $Pd_{E.coli}$, 150 mL of soybean oil (solvent free), $T = 100\,°C$, $pH_2 = 5$ bar, $N = 800$ rpm. ●: C18:0; ▲: *trans*-C18:1; ■: *cis*-C18:1; ◇: *cis*-C18:2; ○: C18:3. b) Comparison of the formation of *cis*-/*trans*-C18:1 and c) C18:0 at the same *cis*-C18:2 conversion by using Pd/Al_2O_3 and bio-$Pd_{E.coli}$. Reaction conditions were: 150 mg of 5 wt% Pd catalysts, 150 mL of soybean oil (solvent free), $T = 100\,°C$, $pH_2 = 5$ bar, $N = 800$ rpm. In b): ♦: bio-$Pd_{E.coli}$, *trans*; ◇: bio-$Pd_{E.coli}$, *cis*; ■: Pd/Al_2O_3 *trans*; □: Pd/Al_2O_3, *cis*. In c): ♦: bio-$Pd_{E.coli}$; ■: Pd/Al_2O_3.

Table 6
A comparison of the component distribution in soybean oil hydrogenations using 5 wt% $Pd_{E.coli}$ and 5 wt% Pd/Al_2O_3, at the reaction time when the highest amount of preferable product *cis*-C18:1 was produced (~5 h for bio-$Pd_{E.coli}$ and ~1 h for Pd/Al_2O_3. Reaction conditions were: 150 mg of 5 wt% Pd catalysts, 150 mL of soybean oil (solvent free), $T = 100\,^{\circ}C$, $pH_2 = 5$ bar, $N = 800$ rpm.

	Component concentration, mol L^{-1}	
	5 wt% $Pd_{E.coli}$	5 wt% Pd/Al_2O_3
Products		
cis-C18:1	1.03 ± 0.04 (at ~5 h)	1.07 ± 0.02 (at ~1 h)
trans-C18:1	0.26 ± 0.03	0.52 ± 0.02
C18:0	0.19 ± 0.00	0.34 ± 0.06
Reactants		
cis-C18:3	0.05 ± 0.02 (78.36 ± 6.10% conversion)	0.04 ± 0.01 (83.15 ± 3.39% conversion)
cis-C18:2	0.97 ± 0.10 (45.52 ± 5.61% conversion)	0.68 ± 0.08 (61.49 ± 4.28% conversion)

centration of 1.03 ± 0.04 mol L^{-1} whereas in the reaction over 5 wt% Pd/Al_2O_3, a maximum yield of *cis*-C18:1 was 1.07 ± 0.02 mol L^{-1} at ~1 h, after which *cis*-C18:1 was consumed *via* the *cis*-*trans* isomerisation, while further saturation of *cis*-C18:1 became dominant. Despite the slower reaction using bio-$Pd_{E.coli}$, for the same amount of *cis*-C18:1 produced, bio-$Pd_{E.coli}$ produced 50% less *trans*-C18:1 than Pd/Al_2O_3 (Table 6). Saturated fatty acid C18:0, was ~ halved in the case of bio-$Pd_{E.coli}$ as compared to Pd/Al_2O_3 (Table 6). When a similar amount of *cis*-C18:2 was converted (~33%; Fig. 6b), 5 wt% $Pd_{E.coli}$ produced ~24% less *trans*-C18:1 than 5 wt% Pd/Al_2O_3 (Fig. 6b) and similarly less saturated C18:0 (Fig. 6c). It is apparent that the higher activity of the Pd/Al_2O_3 catalyst contributed to the formation of *trans*-isomer and the saturated C18:0 at the expense of *cis*-C18:1 (Table 6). Hence, we conclude that conventional Pd/Al_2O_3 catalyst gave less comparative chemoselectivity and lower control over the level of hydrogenation while 5 wt% $Pd_{E.coli}$ appeared to maintain better the production of *cis*-C18:1 while at the same time suppressing the formation of unwanted *trans*-C18:1 and C18:0, albeit at the expense of the overall conversion rate.

It was suggested [41] that the hydrogenation of unsaturated fatty acids is sensitive to the shape, geometry, and size of the metal crystallites. Similar to the observation of a lower production of *trans*-pentene using bio-$Pd_{E.coli}$ (above), a lower yield of *trans*-C18:1 in soybean oil hydrogenation over 5 wt% $Pd_{E.coli}$ can be attributed to its smaller average size of Pd bio-nanoparticles as compared to 5 wt% Pd/Al_2O_3 (4.3 nm and 12.8 nm respectively); these data justify the further examination of the catalytic activity of the biomaterials, although possible contributions of particle shape were not examined.

3.4.3. Comparison of bio-$Pd_{E.coli}$ with bio-$Pd_{D.desulfuricans}$

A comparison of catalytic performance was made between 5 wt% $Pd_{E.coli}$ and 5 wt% $Pd_{D.desulfuricans}$ in soybean oil hydrogenation under the same reaction conditions (Fig. 7a). Both types of bio-Pd gave similar conversions (within error; three independent preparations) of both *cis*-C18:3 and *cis*-C18:2 after 5 h, suggesting a similar mechanism of activity of the two bio-Pd catalysts. In terms of the formation of desired *cis*-C18:1, identical amounts were produced at comparable *cis*-C18:2 conversions (Fig. 7*b*), with identical *trans*-C18:1 formation (Fig. 7c). The molar excess of the *cis*-isomer was ~4-fold (Fig. 7b, c).

Hence, we conclude that related microorganisms produce bio-Pd with such similarity as to have little effect on the catalytic activity between them at a wt% Pd loading of 5% and Bio-$Pd_{E.coli}$ would be the catalyst of choice for commercial development (see Introduction). The question remains as to the nature of the specific differences, both atomic-scale and electronic, between bio-Pd (supported on biochemical ligands) and chemical catalysts (supported on inorganic structures). More detailed studies into the nature of the nanoparticulate catalyst at the cell surface have been carried out using X-ray photoelectron spectroscopy and analytical X-ray methods (EXAFS) (J. Omajali, L.E. Macaskie and M. Merroun, unpublished) which will be reported in full in subsequent publications.

3.4.4. Catalytic activity of bio-Pd made using 'second life' cells of E. coli

E. coli was used to produce hydrogen via the mixed acid fermentation in a primary biohydrogen process [33]. For experiments using 'second life' biomass for catalyst manufacture, the harvested cells were treated with H_2 (Method A) to maintain active the pre-induced enzymes of the mixed acid fermentation pathway responsible for hydrogen production, in particular hydrogenase-3. This enzyme is responsible for hydrogen synthesis via splitting of the toxic product formate into $H_2 + CO_2$ and is also implicated in bio-Pd manufacture, operating in the reverse direction of hydrogen splitting, with electron transfer onto Pd(II) [see 9]. For comparison with the 'purpose-grown' cells in this study a duplicate set of cells was incubated with fumarate/glycerol to place them under conditions of anaerobic respiration (Method B) where formate does not accumulate. Here, hydrogenase-3 is not upregulated and energy-conserving respiratory hydrogenases 1 and 2 would predominate [see 9]. Two key studies have shown that the catalytic activity of the bio-Pd relates to the specific hydrogenase that produced it, using specific mutations in both *E. coli* [9] and in *D. fructosovorans* [10,76].

A. preliminary comparison of the bio-Pd of 'second life' cells (bio-$Pd_{secondlife}$) in the hydrogenation of 2-pentyne showed that the conversion rate was decreased by ~ 6-fold as compared to purpose-grown cells irrespective of the use of Method A or Method B. [57]. In contrast, with soybean oil hydrogenation after 5 h of reaction, the *cis*-C18:2 conversion via the bio-Pd of purpose-grown cells was 45.5 ± 5.6% while that of bio-$Pd_{secondlife}$ was 21% (Method A) and 27% (Method B). Hence the activity of bio-$Pd_{secondlife}$ in soybean oil hydrogenation was proportionally better than for 2-pentyne hydrogenation, showing ~ half of the rate of purpose-grown cells rather than 1/6th.

The selectivity of the soybean oil hydrogenation reaction is shown in Fig. 8. Bio-$Pd_{secondlife}$ made by Method B (anaerobic respiration) showed a slightly higher selectivity as compared to purpose-grown cells, 'trading' the lower reaction rate (see above) for a slightly higher selectivity towards the *cis*-product. Similarly, 'second life' cells that had been maintained under fermentative conditions and pre-treated with H_2 for 30 min prior to palladisation (Method A) gave Pd nanoparticles of enhanced selectivity as compared to purpose-grown cells or bio-$Pd_{secondlife}$ and to those made using Method B (Fig. 8). The main differentiating parameter between the two cell preparations, as specified by their culturing conditions (see above), is the relative activity of hydrogenase-2 (membrane-bound, periplasmic-facing; functions in energy conservation under anaerobic respiration) and hydrogenase-1 (membrane-bound; periplasmic-facing; functions in energy conservation under fermentative conditions) [77] and hydrogenase-3 which splits the fermentation product formate (see

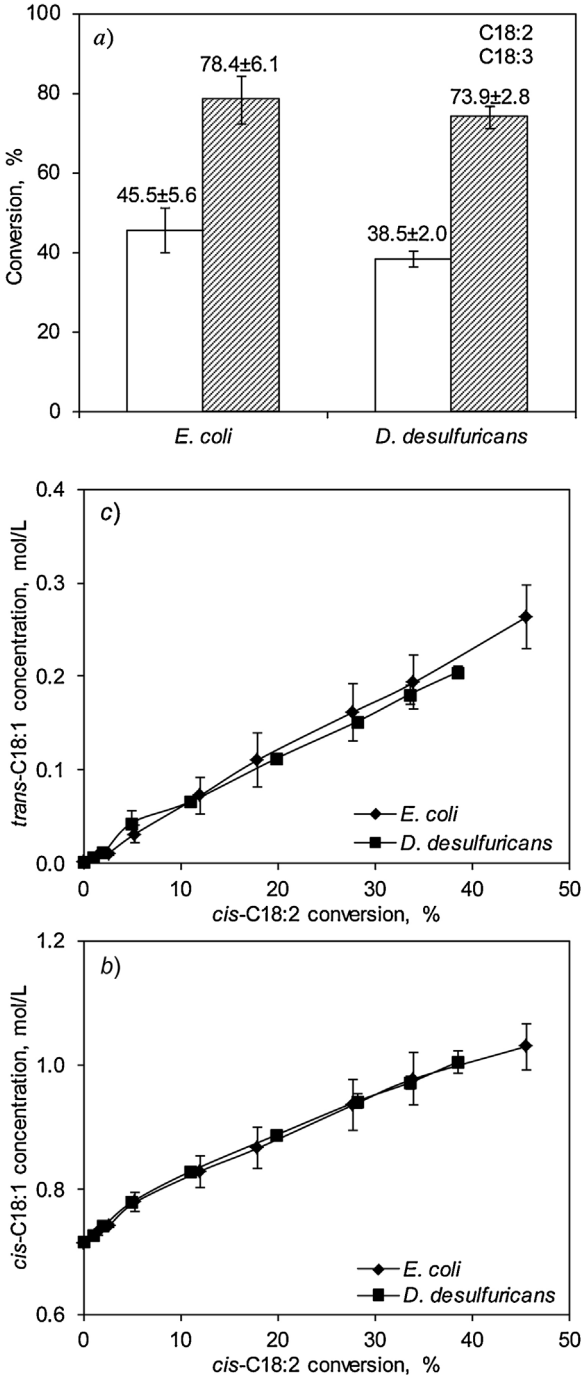

Fig. 7. Comparison of a): the reactant conversion after 5 h and comparison of the formation of b): *cis*-C18:1 and *c)*: *trans*-C18:1 at the same *cis*-C18:2 conversion in soybean oil hydrogenation using bio-$Pd_{E.coli}$ and bio-$Pd_{D.desulfuricans}$. Reaction conditions were: 150 mg of 5 wt% bio-Pd, 150 mL of soybean oil (solvent free), $T = 100\,^{\circ}C$, $pH_2 = 5$ bar, $N = 800$ rpm. ♦: bio-$Pd_{E.coli}$; ■: Bio-$Pd_{D.desulfuricans}$.

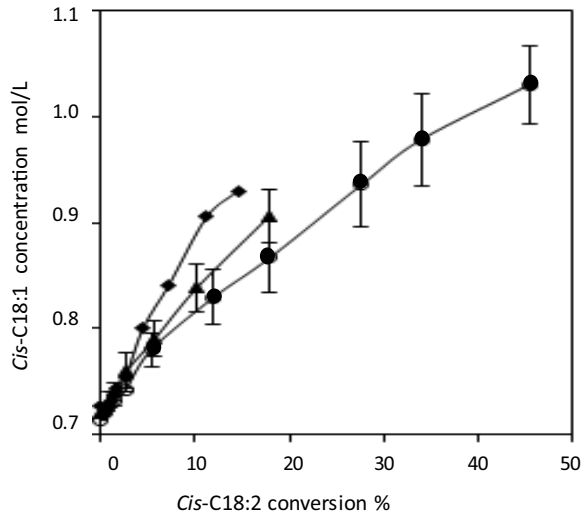

Fig. 8. Use of bio-$Pd_{E.coli}$ made from 'second life' bacteria previously used in a hydrogen production process. Cells were taken from a primary production process (after 3 weeks) as described by Orozco et al. [33]. The harvest was split and treated with H_2 (Method A) or with fumarate (for anaerobic respiration: Method B) with bio-Pd made in each case as for purpose-grown bacteria. The selectivity to *cis*-C18:1 (against *cis*-C18:2 conversion) is shown for: ●, purpose-grown cells (anaerobic respiratory cells); ♦, second life bacteria incubated by Method A (under H_2); ▲, second life bacteria incubated by Method B (anaerobic respiratory cells). Data are mean ±SEM where shown, or the mean from two experiments where the difference between them was less than 10%.

above) and is membrane- bound and cytoplasmic facing [see 9]; previous studies have shown that the orientation, size distribution and "substrate availability" of the Pd-nanoparticles were closely linked to the location and directionality of the Hyd enzyme that was specifically over-expressed during NP production [9,10].

In the reduction of CrO_4^{2-} a mutant with only hydrogenase-3 gave a bio-Pd ~20% as active as the parent strain or a mutant that contained only hydrogenase-1, suggesting that hydrogenase-1 is implicated for making bio-Pd that is best able to reduce CrO_4^{2-}, reflecting its location facing into the hydrated, charged periplasm [9]. However the bio-Pd of a mutant lacking hydrogenase-2 (similarly periplasmically-facing) was compromised similarly to that of bio-Pd from hydrogenase-3 only [9] suggesting that it is not simply the hydrophilicity of both substrate and bio-Pd location which are important.

The 'second life' cells (strain IC007) were a derivative of strain MC4100 that had been engineered for hydrogen overproduction by deletion of the formate hydrogen lyase repressor (*FhlA*) (i.e. upregulation of hydrogenase-3) [33] and their bio-$Pd_{secondlife}$ supported ~3-fold greater power output when used as a fuel cell electrocatalyst supported on activated carbon [33]. A detailed study in hydrogenation reactions has not been done using *E. coli* mutants but Skibar et al. [76] reported a study using a mutant of *D. fructosovorans* lacking its two periplasmic hydrogenases. These cells contained only membrane-bound residual hydrogenase i.e. functionally equivalent to a Hyd-3 only mutant of *E. coli* and both showed the same membrane localisation of cytoplasmically-facing Pd(0)-NPs([9,10]). When tested in the hydrogenation of itaconic acid, the conversion after 10 mins was 25% and 40% for the bio-$Pd_{D.fructosovorans}$ parent and mutant, respectively [76], which is consistent with the key role for hydrogenase-3 in the bio-Pd catalyst production via hydrogenation reactions described here, and is consistent with the membrane-localisation of this enzyme, which may also explain the greater activity of bio-$Pd_{secondlife}$ against the hydrophobic soybean oil than the 2-pentyne which was provided in a carrier of water-miscible isopropanol. The precise factors which govern reaction selectivity in a complex system where bio-Pd is made on multiple sites of varying hydrophobicity and/or occlusion require further development, probably involving a synthetic biology approach and it should also be noted that the access of substrate to the intracellular Pd-NPs was not measured nor the extent to which the acetone wash removed membrane components (acetone treatment is a recognised method of permeabilising cells [78]). It should also be noted that catalytic intracellular bio-Pd NPs are produced by aerobically-grown cells of both *E. coli* [79,80] and *Serratia* sp. [15] which opens the way to using additional types of waste

biomass arising from, for example, recombinant product formation since such cells are grown aerobically to maximise the cell yield.

One key aspect of industrial catalysis which impacts upon process economy is the stability of catalysts with respect to their recovery from the reaction mixture and their re-use in subsequent reactions. Bennett et al. [11] reported that bio-$Pd_{D.desulfuricans}$ retained 95% of its activity over 6 sequential alkyllation reactions whereas a commercial catalyst retained only ~5% of its activity. Bio-$Pd_{E.coli}$ was less stable, losing half of its activity over 4 sequential cycles in the hydrogenation of itaconic acid (A. Tsoligkas, K. Deplanche and L.E. Macaskie, unpublished work), but the same study showed that catalyst stability was retained completely by bio-Pd of *E. coli*, and also by the related *Serratia* sp. by self immobilisation of the bacteria as a biofilm onto a support [81]. The adhesive and cohesive strength were quantified via a micromanipulation method [81] and examination of a flow-through column system by MRI showed no evidence of catalyst loss under load [20].

4. Conclusions

A set of palladium catalysts comprising conventional Pd/Al_2O_3 and two biomass supported bio-Pds, were catalytically active in industrially important hydrogenations of 2-pentyne and soybean oil. Both types of bio-Pd behaved similarly. In the former reaction, 5 wt% $Pd_{E.coli}$ gave a higher production of *cis*-2-pentene in comparison with the commercial catalyst. In soybean oil hydrogenation bio-$Pd_{E.coli}$ showed a slower *cis*-C18:2 conversion than the corresponding conventional Pd/Al_2O_3 but with the advantage of a lower *cis-trans* isomerisation and complete hydrogenation to the unsaturated double bond on its active sites. Hence, biomass-supported precious metal catalyst is an environmentally attractive, 'green' alternative to conventional heterogeneous catalyst for application in industrial hydrogenation processes. In order to impact upon well-established 'traditional' catalysis a new method must be facile, scalable and economic. This study demonstrates that bio-Pd made from 'second life' bacteria from a primary synthetic process outperformed, with respect to product selectivity, 'purpose grown' bacteria in a complex hydrogenation. This would negate the large cost of biomass growth while pioneering the concept of manufacture of 'valuable resources' from wastes while minimising environmental impact.

Acknowledgements

This work was supported by EPSRC grants EP/H029567/1, EP/I007806/1 and EP/J008303/1 and by NERC (grant No NE/L014076/1). Artwork in graphical abstract was from Prof. G.M.Gadd, University of Dundee, UK.

Appendix A. Supplementary data

Supplementary data associated with this article can be found, in the online version, at http://dx.doi.org/10.1016/j.apcatb.2016.05.060.

References

[1] M. Schneider, Online Source: The amazing metal sponge (1995). Pittsburgh Supercomputing Center, Projects in Scientific Computing.
[2] J. Chen, Q.H. Zhang, Y. Wang, H.L. Wan, Adv. Synth. Catal. 350 (2008) 453–464.
[3] W.Y. Yu, M.H. Liu, H.F. Liu, J.M. Zheng, J. Colloid Interface Sci. 210 (1999) 218–221.
[4] D. Berger, G.A. Traistaru, B.S. Vasile, I. Jitaru, C. Matei, Sci. Bull.—Politeh. Univ. Bucharest Ser. B 72 (2010) 113–120.
[5] H.J. Chen, G. Wei, A. Ispas, S.G. Hickey, A. Eychmuller, J. Phys. Chem. C 114 (2010) 21976–21981.
[6] J.A. Bennett, N.J. Creamer, K. Deplanche, L.E. Macaskie, I.J. Shannon, J. Wood, Chem. Eng. Sci. 65 (2010) 282–290.
[7] T. Hennebel, B. De Gusseme, N. Boon, W. Verstraete, Trends Biotechnol. 27 (2009) 90–98.
[8] J.R. Lloyd, P. Yong, L.E. Macaskie, Appl. Environ. Microbiol. 64 (1998) 4607–4609.
[9] K. Deplanche, I. Caldelari, I.P. Mikheenko, F. Sargent, L.E. Macaskie, Microbiology 156 (2010) 2630–2640.
[10] I.P. Mikheenko, M. Rousset, S. Dementin, L.E. Macaskie, Appl. Environ. Microbiol. 74 (2008) 6144–6146.
[11] J.A. Bennett, I.P. Mikheenko, K. Deplanche, I.J. Shannon, J. Wood, L.E. Macaskie, Appl. Catal. B 140 (2013) 700–707.
[12] T.S.A. Heugebaert, S. De Corte, T. Sabbe, T. Hennebel, W. Verstraete, N. Boon, C.V. Stevens, Tetrahedron Lett. 53 (2012) 1410–1412.
[13] N.J. Creamer, I.P. Mikheenko, P. Yong, K. Deplanche, D. Sanyahumbi, J. Wood, K. Pollmann, M. Merroun, S. Selenska-Pobell, L.E. Macaskie, Catal. Today 128 (2007) 80–87.
[14] K. Deplanche, PhD Thesis University of Birmingham: New Nanocatalysts Made by Bacteria from Metal Solutions and Recycling of Metal Wastes, The University of Birmingham, 2008.
[15] K. Deplanche, J.A. Bennett, I.P. Mikheenko, J. Omajali, A.S. Wells, R.E. Meadows, J. Wood, L.E. Macaskie, Appl. Catal. B 147 (2014) 651–665.
[16] K. Deplanche, M.L. Merroun, M. Casadesus, D.T. Tran, I.P. Mikheenko, J.A. Bennett, J. Zhu, I.P. Jones, G.A. Attard, J. Wood, S. Selenska-Pobell, L.E. Macaskie, J. R. Soc. Interface 9 (2012) 1705–1712.
[17] N.J. Creamer, V.S. Baxter-Plant, J. Henderson, M. Potter, L.E. Macaskie, Biotechnol. Lett. 28 (2006) 1475–1484.
[18] M.D. Redwood, K. Deplanche, V.S. Baxter-Plant, L.E. Macaskie, Biotechnol. Bioeng. 99 (2008) 1045–1054.
[19] K. Deplanche, L.E. Macaskie, Biotechnol. Bioeng. 99 (2008) 1055–1064.
[20] D.A. Beauregard, P. Yong, L.E. Macaskie, M.L. Johns, Biotechnol. Bioeng. 107 (2010) 11–20.
[21] A.N. Mabbett, D. Sanyahumbi, P. Yong, L.E. Macaskie, Environ. Sci. Technol. 40 (2006) 1015–1021.
[22] K. Deplanche, A.J. Murray, C. Mennan, S. Taylor, L.E. Macaskie, Biorecycling of precious metals and rare earth elements, in: M.M. Rahman (Ed.), Nanomaterials, InTech, 2011, pp. 279–314.
[23] D. McDonald, L.B. Hunt, The Growth of Industrial Catalysis with the Platinum Metals, A History of Platinum and Its Allied Metals, The Priory Press, Hertfordshire, 1982, pp. 385–402.
[24] V. Baxter-Plant, I.P. Mikheenko, L.E. Macaskie, Biodegradation 14 (2003) 83–90.
[25] S. Harrad, M. Robson, S. Hazrati, V.S. Baxter-Plant, K. Deplanche, M.D. Redwood, L.E. Macaskie, J. Environ. Monit. 9 (2007) 314–318.
[26] B. Mertens, C. Blothe, K. Windey, W. De Windt, W. Verstraete, Chemosphere 66 (2007) 99–105.
[27] A.N. Mabbett, P. Yong, J.P.G. Farr, L.E. Macaskie, Biotechnol. Bioeng. 87 (2004) 104–109.
[28] A.C. Humphries, I.P. Mikheenko, L.E. Macaskie, Biotechnol. Bioeng. 94 (2006) 81–90.
[29] L.E. Macaskie, A.C. Humphries, I.P. Mikheenko, V.S. Baxter-Plant, K. Deplanche, M.D. Redwood, J.A. Bennett, J. Wood, J. Chem. Technol. Biotechnol. 87 (2012) 1430–1435.
[30] P. Yong, M. Paterson-Beedle, I.P. Mikheenko, L.E. Macaskie, Biotechnol. Lett. 29 (2007) 539–544.
[31] I.P. Mikheenko, PhD Thesis University of Birmingham: Nanoscale Palladium Recovery, The University of Birmingham, 2004.
[32] N.J. Creamer, K. Deplanche, T.J. Snape, I.P. Mikheenko, P. Yong, D. Samyahumbi, J. Wood, K. Pollmann, S. Selenska-Pobell, L.E. Macaskie, Hydrometallurgy 94 (2008) 138–143.
[33] R.L. Orozco, M.D. Redwood, P. Yong, I. Caldelari, F. Sargent, L.E. Macaskie, Biotechnol. Lett. 32 (2010) 1837–1845.
[34] H.J. Beckmann, J. Am. Oil Chem. Soc. 60 (1983) 282–290.
[35] R. Larsson, J. Am. Oil Chem. Soc. 60 (1983) 275–281.
[36] H.B.W. Patterson, Hydrogenation of Fats and Oils, Applied Science Publishers Ltd., 1983.
[37] B. Nohair, C. Especel, P. Marecot, C. Montassier, L.C. Hoang, J. Barbier, C.R. Chim. 7 (2004) 113–118.
[38] B. Nohair, C. Especel, G. Lafaye, P. Marecot, L.C. Hoang, J. Barbier, J. Mol. Catal. A: Chem. 229 (2005) 117–126.
[39] C.M. Oomen, M.C. Ocke, E.J.M. Feskens, M.A.J. van Erp-Baart, F.J. Kok, D. Kromhout, Lancet 357 (2001) 746–751.
[40] M.B. Fernandez, J.F. Sanchez, G.M. Tonetto, D.E. Damiani, Chem. Eng. J. 155 (2009) 941–949.
[41] M. Plourde, K. Belkacemi, J. Arul, Ind. Eng. Chem. Res. 43 (2004) 2382–2390.
[42] K. Belkacemi, A. Boulmerka, J. Arul, S. Hamoudi, Top. Catal. 37 (2006) 113–120.
[43] K. Belkacemi, S. Hamoudi, Ind. Eng. Chem. Res. 48 (2009) 1081–1089.
[44] A. Bernas, J. Myllyoja, T. Salmi, D.Y. Murzin, Appl. Catal. A 353 (2009) 166–180.
[45] A. Molnar, A. Sarkany, M. Varga, J. Mol. Catal. A: Chem. 173 (2001) 185–221.
[46] P. Yong, N.A. Rowson, J.P.G. Farr, I.R. Harris, L.E. Macaskie, J. Chem. Technol. Biotechnol. 77 (2002) 593–601.
[47] K. Deplanche, I.P. Mikheenko, J.A. Bennett, M. Merroun, H. Mounzer, J. Wood, L.E. Macaskie, Top. Catal. 54 (2011) 1110–1114.
[48] J. Horiuti, M. Polanyi, Trans. Faraday Soc. 30 (1934) 1164–1172.
[49] A.L. Patterson, Phys. Rev. 56 (1939) 978–982.
[50] J. Omajali, I.P. Mikheenko, M.L. Merroun, J. Wood, L.E. Macaskie, J. Nanaopart. Res. 17 (2015) 1–17.
[51] L. Cerveny, V. Ruzicka, Catal. Rev.: Sci. Eng. 24 (1982) 503–566.

[52] L. Cerveny, Chem. Eng. Commun. 83 (1989) 31–63.
[53] X.C. Guo, R.J. Madix, J. Catal. 155 (1995) 336–344.
[54] T. Ouchaib, J. Massardier, A. Renouprez, J. Catal. 119 (1989) 517–520.
[55] P. Sautet, J.F. Paul, Catal. Lett. 9 (1991) 245–260.
[56] M. Varga, A. Molnar, M. Mohai, I. Bertoti, M. Janik-Czachor, A. Szummer, Appl. Catal. A 234 (2002) 167–178.
[57] J. Zhu, Synthesis of Precious Metal Nanoparticles Supported on Bacterial Biomass for Catalytic Applications in Chemical Transformations PhD Thesis, The University of Birmingham, UK, 2014.
[58] J. Wood, L. Bodenes, J. Bennett, K. Deplanche, L.E. Macaskie, Ind. Eng. Chem. Res. 49 (2010) 980–988.
[59] A. Bruehwiler, N. Semagina, M. Grasemann, A. Renken, L. Kiwi-Minsker, A. Saaler, H. Lehmann, W. Bonrath, F. Roessler, Ind. Eng. Chem. Res. 47 (2008) 6862–6869.
[60] M.L. Toebes, J.A. van-Dillen, K.P. de-Jong, J. Mol. Catal. A: Chem. 173 (2001) 75–98.
[61] I.V. Deliy, N.V. Maksimchuk, R. Psaro, N. Ravasio, V. Dal Santo, S. Recchia, E.A. Paukshtis, A.V. Golovin, V.A. Semikolenov, Appl. Catal. A 279 (2005) 99–107.
[62] M.B. Smith, March's Advanced Organic Chemistry: Reactions, Mechanisms, and Structure, Wiley, 2013.
[63] G.H. Jonker, PhD Thesis University of Birmingham: Hydrogenation of Edible Oils and Fats, University of Groningen, The Netherlands, 1999.
[64] M.B. Fernandez, G.M. Tonetto, G.H. Crapiste, D.E. Damiani, J. Food Eng. 82 (2007) 199–208.
[65] M.Y. Chang, B.I. Morsi, Chem. Eng. Sci. 47 (1992) 1779–1790.
[66] B. Fillion, B.I. Morsi, Ind. Eng. Chem. Res. 39 (2000) 2157–2168.
[67] M.Y. Chang, B.I. Morsi, Chem. Eng. Sci. 46 (1991) 2639–2650.
[68] L. Bern, M. Hell, N.H. Schöön, J. Am. Oil Chem. Soc. 52 (1975) 391–394.
[69] R.V. Chaudhari, M.G. Parande, P.A. Ramachandran, P.H. Brahme, H.G. Vadgaonkar, R. Jaganathan, AIChE J. 31 (1985) 1891–1903.
[70] E. Santacesaria, P. Parrella, M.S. Diserio, G. Borrelli, Appl. Catal. A 116 (1994) 269–294.
[71] A.F. Perez-Cadenas, F. Kapteijn, M.M.P. Zieverink, J.A. Moulijn, Catal. Today 128 (2007) 13–17.
[72] B. Fillion, B.I. Morsi, K.R. Heier, R.M. Machado, Ind. Eng. Chem. Res. 41 (2002) 697–709.
[73] A.J. Dijkstra, Eur. J. Lipid Sci. Technol. 114 (2012) 985–998.
[74] A.J. Haighton, K. Vanputte, L.F. Vermaas, J. Am. Oil Chem. Soc. 49 (1972) 153–156.
[75] A.E. Bailey, Bailey's Industrial Oil and Fat Products, John Wiley & Sons, New York, 1979.
[76] W. Skibar, L.E. Macaskie, W. Pompe, I. Jäger, S. Selenska-Pobell, M. Rousset, C. Cances, J. Hofinger, Final Report EU Contract G5-RD-CT-2002-00750, The European Commission, Brussels, 2005.
[77] R.G. Sawers, S.P. Ballantine, D.H. Boxer, J. Bacteriol. 164 (1985) 1324–1331.
[78] B.S. Brown, Biological Membranes Curriculum Guidance for Advanced Biology, The Biochemical Society, 1996.
[79] J.M. Foulkes, K.S. Malone, V. Coker, N.J. Turner, J.R. Lloyd, ACS Catal. 1 (2011) 1589–1594.
[80] J.M. Foulkes, K. Deplanche, F. Sargent, L.E. Macaskie, J.R. Lloyd, Geomicrobiol. J. 33 (2016) 230–236.
[81] P. Yong, W. Liu, Z. Zhang, M.L. Johns, L.E. Macaskie, Biotechnol. Lett. 37 (2015) 2181–2191.